

# Bag of Tricks for Training Deeper Graph Neural Networks: A Comprehensive Benchmark Study

Tianlong Chen<sup>‡</sup>, Kaixiong Zhou<sup>‡</sup>, Keyu Duan, Wenqing Zheng, Peihao Wang, Xia Hu, and Zhangyang Wang

**Abstract**—Training deep graph neural networks (GNNs) is notoriously hard. Besides the standard plights in training deep architectures such as vanishing gradients and overfitting, it also uniquely suffers from over-smoothing, information squashing, and so on, which limits their potential power for encoding the high-order neighbor structure in large-scale graphs. Although numerous efforts are proposed to address these limitations, such as various forms of skip connections, graph normalization, and random dropping, it is difficult to disentangle the advantages brought by a deep GNN architecture from those “tricks” necessary to train such an architecture. Moreover, the lack of a standardized benchmark with fair and consistent experimental settings poses an almost insurmountable obstacle to gauge the effectiveness of new mechanisms. In view of those, we present the first fair and reproducible benchmark dedicated to assessing the “tricks” of training deep GNNs. We categorize existing approaches, investigate their hyperparameter sensitivity, and unify the basic configuration. Comprehensive evaluations are then conducted on tens of representative graph datasets including the recent large-scale Open Graph Benchmark, with diverse deep GNN backbones. We demonstrate that an organic combo of initial connection, identity mapping, group and batch normalization attains the new state-of-the-art results for deep GNNs on large datasets. Codes are available: [https://github.com/VITA-Group/Deep\\_GCN\\_Benchmarking](https://github.com/VITA-Group/Deep_GCN_Benchmarking).

**Index Terms**—Deep Graph Neural Networks, Over-smoothing, Training Technique, Benchmark

## 1 INTRODUCTION

GRAPH neural networks (GNNs) [1] are powerful tools for modeling graph-structured data, and have been widely adopted in various real-world scenarios, including inferring individual relations in social and academic networks [2], [3], [4], [5], [6], [7], [8], [9], [10], improving predictions of recommendation systems [3], [11], [12], augmenting signal processing and communication [13], [14], [15], modeling proteins for drug discovery [16], [17], segmenting large point clouds [18], [19], among others. While many classical GNNs have no more than just a few layers, recent advances attempt to investigate deeper GNN architectures [19], [20], [21]. There are massive examples on which deeper GNNs help, such as “geometric” graphs representing structures of molecules, point clouds [19], or meshes [22]. Deeper architectures are also found with superior performance on large-scale graphs like the latest Open Graph Benchmark (OGB) [23].

However, training deep GNNs is notoriously challenging [19]. Besides the standard plights in training deep architectures such as *vanishing gradients* and *overfitting*, the training of deep GNNs suffers several unique barriers that limit their potential power on the large-scale graphs. One of them is *over-smoothing*, i.e., the node features tending to become indistinguishable as the result of performing several recursive neighborhood aggregation [24], [25], [26], [27]. This

behavior was first observed in GCN models [25], [26], which acts similarly to low-pass filters, and prevents deep GNNs from effectively modeling the higher-order dependencies from multi-hop neighbors. Another phenomenon is the *bottleneck* phenomenon: while deep GNNs are expected to utilize longer-range interactions, the structure of graph often results in the exponential growth of receptive field, causing “over-squashing” of information from the exponentially increasing neighbours into fixed-size vectors [28], and explaining why some deep GNNs do not improve in performance compared to their shallower peers.

To address the aforementioned roadblocks, typical approaches could be categorized as *architectural modifications*, and *regularization & normalization*: both we view as “training tricks”. The former includes various types of residual connections [19], [25], [29], [30], [30], [31], [31], [32], [33]; and the latter include random edge dropping [34], [35], pairwise distance normalization between node features (PairNorm) [36], node-wise mean and variance normalization (NodeNorm) [37], among many other normalization options [27], [38], [39], [40], [41], [42]. While these techniques in general contribute to effective training of deep GNNs with tens of layers, their gains are not always significant nor consistent [37]. Furthermore, it is often non-straightforward to disentangle the gain by deepening the GNN architecture, from the “tricks” necessary to train such a deeper architecture. In some extreme situations, contrary to the initial belief, newly proposed training techniques could improve shallower GNNs even to outperform deep GNNs [37], making our pursuit of depth unpersuasive. Those observations have shed light on a **missing key knob** on studying deep GNNs: we lack a standardized benchmark that could offer fair and consistent comparison on the effectiveness of deep

- Tianlong Chen, Wenqing Zheng, Peihao Wang and Zhangyang Wang are with the Department of Electrical and Computer Engineering, The University of Texas at Austin, TX, 78712. E-mail: {tianlong.chen, w.zheng, peihaowang, atlaswang}@utexas.edu
- Kaixiong Zhou, Keyu Duan and Xia Hu are with the Department of Computer Science, Rice University. E-mail: {kz34, k.duan, xia.hu}@rice.edu
- <sup>‡</sup> indicates the equal contribution. Correspondence to Zhangyang Wang (atlaswang@utexas.edu).

GNN training techniques. Without isolating the effects of deeper architectures from their training “tricks”, one might never reach convincing answers whether deep graph neural networks with *ceteris paribus* should perform better.

## 1.1 Our Contributions

Aiming to establish such a fair benchmark, our first step is to thoroughly investigate the design philosophy and implementation details on dozens of popular deep GNN training techniques, including various residual connections, graph normalization, and random dropping. The summarization could be found in Tables 1, 12, 13, and 14. Somehow unfortunately, we find that even sticking to the same dataset and GNN backbone, the hyperparameter configurations (e.g., hidden dimension, learning rate, weight decay, dropout rate, training epochs, early stopping patience) are highly inconsistently implemented, often varying case-to-case, which make it troubling to draw any fair conclusion.

To this end, in this paper we carefully examine those sensitive hyperparameters and unify them into one “sweetpoint” hyperparameter set, to be adopted by all experiments. Such lays the foundation for a fair and reproducible benchmark of training deep GNN. Then, we comprehensively explore the diverse combinations of the available training techniques, over *tens of* classical graph datasets with commonly used deep GNN backbones. Our comprehensive study turns out to be worthy. We conclude the baseline training configurations with the superior combo of training tricks, that lead us to attaining the new state-of-the-art results across multiple representative graph datasets including OGB. Specifically, we show that an organic combination of initial connection, identity mapping, group and batch normalizations has preferably strong performance on large datasets.

Our experiments also reveals a number of “surprises”. For example, ❶ as we empirically show, while initial connection [29] and jumping connection [32] are both “beneficial” training tricks when applied alone, combining them together deteriorates deep GNN performance. ❷ Although dense connection brings considerable improvement on large-scale graphs with deep GNNs, it sacrifices the training stability to a severe extent. ❸ As another example, the gain from NodeNorm [37] becomes diminishing when applied to the large-scale datasets or deeper GNN backbones. ❹ Moreover, using random dropping techniques alone often yield unsatisfactory performance. ❺ Lastly, we observe that adopting initial connection and group normalization is universally effective across tens of classical graph datasets. Those findings urge more synergistic rethinking of those seminal works.

## 2 RELATED WORKS

### 2.1 Graph Neural Networks and Training Deep GNNs

GNNs [7], [12], [43], [44], [45], [46], [47], [48], [49], [50], [51], [52] have established state-of-the-art results on various tasks [6], [10], [44], [46], [53], [54], [55]. There are also numerous GNN variants [11], [44], [45], [56], [57], [58], [59], [60], [61], [62], [63], [64]. For example, Graph Convolutional Networks (GCNs) are widely adopted, which can be divided into spectral domain based methods [44], [65] and spatial domain bases methods [59], [66]. Recent effort summarizes a series of useful tricks (e.g., label usage and loss function) to train

shallow GNNs [67], which is different to the deep GNNs benchmark investigated in this paper.

Unlike other deep architectures, not every useful GNN has to be deep. For example, many graphs like social networks, are “small-world” [68], i.e., one node can reach any other node in a few hops. Hereby, adding more layers does not help model over those graphs since the receptive fields of just stacking a few layers would already suffice to provide global coverage. Many predictions in practice, such as in social networks, also mainly rely on short-range information from the local neighbourhood of a node. On the other hand, when the graph data is large in scale, does not have small-world properties, or its task requires long-range information to make prediction, then *deeper GNNs do become necessary*. Examples include molecular graphs, as a molecule’s chemical properties can depend on the atom combination at its opposite sides [69]. The graphs with larger diameters (e.g., citation networks), point clouds or meshes also benefit from GNN depth to capture a whole object and its context [19], [22], [70].

With the prosperity of GNNs, understanding their training mechanism and limitation is of remarkable interest. As GNNs stack spatial aggregations recursively [1], [59], the node representations will collapse to indistinguishable vectors [24], [26], [71]. Such over-smoothing phenomenon hinders the training of deep GNNs and the dependency modeling to high-order neighbors. Specifically, the over-smoothing usually arises when we naively increase the number of graph convolutional layers, which substantially decreases the discriminative power of node embeddings and ends up with a degraded performance on graph learning tasks like node classification and link prediction. Recently, there has been a series of techniques developed to relieve the over-smoothing issue, including *skip connection*, *graph normalization*, *random dropping*. They will be detailed next.

### 2.2 Skip Connection

Motivated by ResNets [72], the skip connection was applied to GNNs to exploit node embeddings from the preceding layers, to relieve the over-smoothing issue. There are several skip connection patterns in deep GNNs, including: (1) residual connection connecting to the last layer [19], [25], (2) initial connection connecting to the initial layer [29], [30], [31], (3) dense connection connecting to all the preceding layers [19], [25], [73], [74], and (4) jumping connection combining all the preceding layers only at the final graph convolutional layer [32], [33]. Note that the last one of jumping connection is a simplified version of dense connection by omitting the complex skip connections at the intermediate layers.

### 2.3 Graph Normalization

A series of normalization techniques has been developed for deep GNNs, including batch normalization (BatchNorm) [38], pair normalization (PairNorm) [36], node normalization (NodeNorm) [37], mean normalization (MeanNorm) [41], differentiable group normalization (GroupNorm) [42], and more. Their common mechanism is to re-scale node embeddings over an input graph to constrain pairwise node distance and thus alleviate over-smoothing. While BatchNorm and PairNorm normalize the whole input graph, GroupNorm first clusters node into groups and then normalizes each

TABLE 1

Configurations of basic hyperparameters adopted to implement different approaches for training deep GNNs on Cora [44]. Other graph datasets are refer to Section A.

Methods	Total epoch	Learning rate & Decay	Weight decay	Dropout	Hidden dimension
Chen et al. (2020) [29]	100	0.01	$5 \times 10^{-4}$	0.6	64
Xu et al. (2018) [32]	-	0.005	$5 \times 10^{-4}$	0.5	{16, 32}
Klicpera et al. (2018) [30]	10000	0.01	$5 \times 10^{-3}$	0.5	64
Zhang et al. (2020) [31]	1500	{0.001, 0.005, 0.01}	-	{0.1, 0.2, 0.3, 0.4, 0.5}	64
Luan et al. (2019) [74]	3000	$1.66 \times 10^{-4}$	$1.86 \times 10^{-2}$	0.65277	1024
Liu et al. (2020) [33]	100	0.01	0.005	0.8	64
Zhao et al. (2019) [36]	1500	0.005	$5 \times 10^{-4}$	0.6	32
Min et al. (2020) [75]	200	0.005	0	0.9	-
Zhou et al. (2020) [42]	1000	0.005	$5 \times 10^{-4}$	0.6	-
Zhou et al. (2020) [37]	50	0.005	$1 \times 10^{-5}$	0	-
Rong et al. (2020) [34]	400	0.01	$5 \times 10^{-3}$	0.8	128
Zou et al. (2020) [76]	100	0.001	-	-	256
Hasanzadeh et al. (2020) [77]	2000	0.005	$5 \times 10^{-3}$	0	128

TABLE 2

The ‘‘sweet point’’ hyperparameter configuration we used on representative datasets.

Settings	Cora	Citeseer	PubMed	OGBN-ArXiv
{Learning rate, Weight decay, Dropout, Hidden dimension}	{0.005, $5 \times 10^{-4}$ , 0.6, 64}	{0.005, $5 \times 10^{-4}$ , 0.6, 256}	{0.01, $5 \times 10^{-4}$ , 0.5, 256}	{0.005, 0, 0.1, 256}

group independently. NodeNorm and MeanNorm operate on each node by re-scaling the associated node embedding with its standard deviation and mean values, respectively.

## 2.4 Random Dropping

Dropout [78] refers to randomly dropping hidden units in a neural network with a pre-fixed probability, which effectively prevents over-fitting. Similar ideas have been inspired for GNNs. DropEdge [34] and DropNode [35] have been proposed to randomly remove a certain number of edges or nodes from the input graph at each training epoch. Alternatively, they could be regarded as data augmentation methods, helping relieve both the over-fitting and over-smoothing issues in training very deep GNNs.

Besides the above widely-adopted tricks of skip connection, graph normalization, and random dropping, there exist some extra efforts made to optimize deep GNNs from other architectural perspectives. For example, the feature over-correlation is relieved to encourage deep GNNs to produce node embeddings with less redundant information [79], [80]. The grouped reversible graph connections and weight sharing among layers are leveraged to reduce memory complexity and train GNNs up to 1,000 layers [81]. Contrastive learning is used to generate the discriminative node representations and relieve the over-smoothing [82]. Similar to SGC [83] and DAGNN [33], DGMLP [84] has been proposed to establish deep GNNs by decoupling the graph convolutions and feature transformation.

## 3 A FAIR AND SCALABLE STUDY OF TRICKS

### 3.1 Prerequisite: Unifying the Hyperparameter Configuration

We carefully examine previous implementations of deep GNNs [29], [30], [32], [33], [34], [36], [37], [42], [74], [75], and list all their basic hyperparameters in Table 1, 12, 13, 14. Those hyperparameters play significant roles in those methods’ achievable performance, but their inconsistency challenges fair comparison of training techniques, which has been traditionally somehow overlooked in literature.

We tune them all with an exhaustive grid search, and identify the most common and effective setting as in Table 2, by choosing the configuration that performs the best across diverse backbones with different layers on the corresponding dataset. That configuration includes learning rate, weight decay, dropout rate, and the hidden dimension of multilayer perceptrons (MLP) in GNNs. We recommend it as a ‘‘sweet point’’ hyperparameter configuration, and strictly follow it in our experiments.

For all experiments, deep GNNs are trained with a maximum of 1000 epochs with an early stop patience of 100 epochs. *One hundred independent repetitions* are conducted for each experiment, and the average performances with the standard deviations of the node classification accuracies are reported in Table 3, 16, 4, 17, 5, 18, 19, and 20. We perform a comprehensive benchmark study of dozens of training approaches on four classical datasets, i.e., Cora, Citeseer, PubMed [44], and OGBN-ArXiv [23] with 2/16/32 layers GCN [44] and simple graph convolutional (SGC) [83] backbones. GCN and SGC are chosen in our work because they are two most common backbone architectures for deep GNNs researches, following the standard in [19], [25], [30], [31], [32], [33], [34], [35], [38], [39], [41], [42], [65], [73], [78], [85], [86]. More details of these benchmark datasets and GNN backbones are collected in Appendix B. The Pytorch framework and Pytorch Geometric [87] are used for all of our implementations. Specific setups for each group of training techniques are included in Section 3.2, 3.3, and 3.4.

### 3.2 Skip Connection

**Formulations.** Skip connections [19], [25], [29], [30], [31], [32], [33] alleviate the vanishing gradient and over-smoothing, and substantially improve the accuracy and stability of training deep GNNs. Let  $\mathcal{G} = (\mathbf{A}, \mathbf{X})$  denotes the graph data, where  $\mathbf{A} \in \mathbb{R}^{n \times n}$  represents the adjacent matrix,  $\mathbf{X} = [\mathbf{x}_1, \mathbf{x}_2, \dots, \mathbf{x}_n]^\top \in \mathbb{R}^{n \times d}$  is the corresponding input node features,  $n$  is the number of nodes in the graph  $\mathcal{G}$ , and  $d$  is the dimension of each node feature  $\mathbf{x}_i$ . In the adjacent matrix  $\mathbf{A}$ , the values of entries can be weighted, i.e.,  $\mathbf{A}_{i,j} \in (0, 1)$ . For a  $L$ -layer GNN, we can apply various

TABLE 3

Test accuracy (%) under different skip connection mechanisms. Experiments are conducted on Cora, Citeseer, PubMed, and OGBN-ArXiv with 2/16/32 layers GCN and SGC. Performance are averaged from 100 independent repetitions, and their standard deviation are presented in Table 16.

Backbone	Settings	Cora			Citeseer			PubMed			OGBN-ArXiv		
		2	16	32	2	16	32	2	16	32	2	16	32
GCN	Residual	74.73	20.05	19.57	66.83	20.77	20.90	75.27	38.84	38.74	70.19	69.34	65.09
	Initial	79.00	<b>78.61</b>	<b>78.74</b>	70.15	<b>68.41</b>	<b>68.36</b>	77.92	<b>77.52</b>	<b>78.18</b>	70.16	70.50	70.23
	Jumping	80.98	76.04	75.57	69.33	58.38	55.03	77.83	75.62	75.36	<b>70.24</b>	<b>71.83</b>	<b>71.87</b>
	Dense	77.86	69.61	67.26	66.18	49.33	41.48	72.53	69.91	62.99	70.08	71.29	70.94
	None	<b>82.38</b>	21.49	21.22	<b>71.46</b>	19.59	20.29	<b>79.76</b>	39.14	38.77	69.46	67.96	45.48
SGC	Residual	<b>81.77</b>	82.55	80.14	71.68	71.31	71.00	78.87	79.86	79.07	69.09	66.52	61.83
	Initial	81.40	<b>83.66</b>	83.77	71.60	<b>72.16</b>	<b>72.25</b>	<b>79.11</b>	79.73	79.74	68.93	69.24	69.15
	Jumping	77.75	83.42	<b>83.88</b>	69.96	71.89	71.88	<b>77.42</b>	<b>79.99</b>	<b>80.07</b>	68.76	70.61	70.65
	Dense	77.31	81.24	77.66	70.99	67.75	66.35	77.12	72.77	74.84	<b>69.39</b>	<b>71.42</b>	<b>71.52</b>
	None	79.31	75.98	68.45	<b>72.31</b>	71.03	61.92	78.06	69.18	66.61	61.98	41.58	34.22

types of skip connections after certain graph convolutional layers with the current and preceding embeddings  $\mathbf{X}^l$ ,  $0 \leq l \leq L$ . Four representative types of skip connections are investigated:

★ *Residual Connection*. [19], [25]

$$\mathbf{X}^l = (1 - \alpha) \cdot \mathbf{X}^l + \alpha \cdot \mathbf{X}^{l-1}.$$

★ *Initial Connection*. [29], [30], [31]

$$\mathbf{X}^l = (1 - \alpha) \cdot \mathbf{X}^l + \alpha \cdot \mathbf{X}^0.$$

★ *Dense Connection*. [19], [25], [73], [74]

$$\mathbf{X}^l = \text{COM}(\{\mathbf{X}^k, 0 \leq k \leq l\}).$$

★ *Jumping Connection*. [32], [33]

$$\mathbf{X}^L = \text{COM}(\{\mathbf{X}^k, 0 \leq k \leq L\}).$$

Here  $\alpha$  in *residual* and *initial connections* is a hyperparameter to weigh the contributions of node features from the current layer  $l$  and previous layers. In our case, the values of best performing  $\alpha$  are searched from  $\{0.1, 0.2, 0.4, 0.6, 0.8\}$  for each experiment. The initial embedding  $\mathbf{X}^0$  is given by  $\mathbf{X}$ . *Jumping connection* as a simplified case of *dense connection* is only applied at the end of whole forward propagation process to combine the node features from all previous layers.

We lastly introduce the combination functions COM used in dense and jumping connections: ① *Concat*,  $\mathbf{X}^l = \text{MLP}([\mathbf{X}^0, \mathbf{X}^1, \dots, \mathbf{X}^l])$ ; ② *Maxpool*,  $\mathbf{X}^l = \text{max}(\text{stack}([\mathbf{X}^0, \mathbf{X}^1, \dots, \mathbf{X}^l]))$ , the operation *max* returns the maximum value for each dimension of a node feature vector; ③ *Attention*,  $\mathbf{X}^l = \text{squeeze}(\mathbf{S}\hat{\mathbf{X}})$ ,  $\mathbf{S} = \sigma(\text{MLP}(\mathbf{X}))$ ,  $\hat{\mathbf{X}} = \text{stack}([\mathbf{X}^0, \mathbf{X}^1, \dots, \mathbf{X}^l])$ .  $\sigma(\cdot)$  is the activation function where *sigmoid* is usually adopted [32], [33]. *stack* and *squeeze* are utilized to rearrange the data dimension so that dimension can be matched throughout the computation. Note that, for every dense connection and jumping connection experiment, we examine all three options for COM in the set  $\{\text{Concat}, \text{Maxpool}, \text{Attention}\}$  and report the one attaining the best performance.

**Experimental observations.** From Table 3 and 16, we can draw the following observations: (i) In general, the initial and jumping connection perform relatively better than the others, especially for training very deep GNNs (i.e.,  $\geq 16$  layers). It demonstrates that these two skip connections more effectively mitigate the over-smoothing issue, assisting graph neural networks going deeper. (ii) For shallow GCN backbones (e.g., 2 layers), using skip connections can incur performance degradation, yet becomes beneficial on the large-scale OGBN-ArXiv dataset. Meanwhile, SGC backbones benefit from skip connections in most of the cases. (iii)

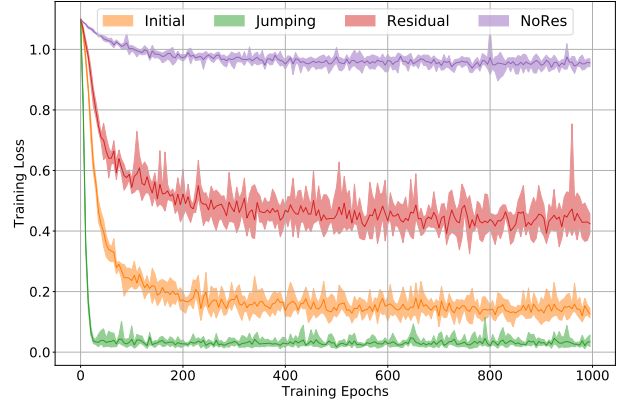


Fig. 1. Training loss under different skip connections on PubMed with 16 layers SGC. Dense connection is omitted due to different scales of loss magnitude. More are included in Section C.

Residual connection only works for 2-layer SGC on Cora. Although the residual connection also brings in shortcuts, its effects to overcome over-smoothing are diminished by increasing depth or growing dataset size, presumably due to its more “local” information flow (only from the preceding one layer), compared to initial and dense connections whose information flows can be directly imported from much earlier layers. (iv) Although the dense connection on average brings significant accuracy improvements on OGBN-ArXiv with SGC, it sacrifices the training stability and leads to considerable performance variance, as consistently shown by Table 16. (v) Figure 1 reveals that skip connections substantially accelerate the training of deep GNNs, which is aligned with the analysis by concurrent work [85].

### 3.3 Graph Normalization

**Formulations.** Graph normalization mechanisms [36], [37], [38], [39], [40], [41], [42] are also designed to tackle over-smoothing. Nearly all graph normalization techniques are applied upon the intermediate node embedding matrix, after passing through several graph convolutions. We use  $\mathbf{X}^l = [\mathbf{x}_1^l, \mathbf{x}_2^l, \dots, \mathbf{x}_n^l]^T \in \mathbb{R}^{n \times d}$  to denote the node embedding matrix at layer  $l$ , where  $\mathbf{x}_i^l \in \mathbb{R}^{d \times 1}$  (we omit  $l$  in later descriptions for notation’s simplicity). Correspondingly,  $\mathbf{x}_{(k)} \in \mathbb{R}^{n \times 1}$  represents the  $k$ -th column of  $\mathbf{X}$ , recording values of the  $k$ -th dimension of each feature embedding.

Our investigated normalization mechanisms are formally depicted as follows:

★ *PairNorm*. [36]

$$\tilde{\mathbf{x}}_i = \mathbf{x}_i - \frac{1}{n} \sum_{i=1}^n \mathbf{x}_i, \text{PairNorm}(\mathbf{x}_i; s) = \frac{s \cdot \tilde{\mathbf{x}}_i}{\sqrt{\frac{1}{n} \sum_{i=1}^n \|\tilde{\mathbf{x}}_i\|_2^2}}.$$

TABLE 4

Test accuracy (%) under different graph normalizations. Experiments are conducted on Cora, Citeseer, PubMed, and OGBN-ArXiv with 2/16/32 layers GCN and SGC. Performance are averaged from 100 independent repetitions, and their standard deviation are presented in Table 17.

Backbone	Settings	Cora			Citeseer			PubMed			OGBN-ArXiv		
		2	16	32	2	16	32	2	16	32	2	16	32
GCN	BatchNorm	69.91	61.20	<b>29.05</b>	46.27	26.25	21.82	67.15	58.00	55.98	70.44	70.52	68.74
	PairNorm	74.43	<b>55.75</b>	17.67	63.26	<b>27.45</b>	20.67	75.67	71.30	61.54	65.74	65.37	63.32
	NodeNorm	79.87	21.46	21.48	68.96	18.81	19.03	78.14	40.92	40.93	70.62	70.75	29.94
	MeanNorm	<b>82.49</b>	13.51	13.03	70.86	16.09	7.70	78.68	18.92	18.00	69.54	70.40	56.94
	GroupNorm	82.41	41.76	27.20	71.30	26.77	<b>25.82</b>	<b>79.78</b>	<b>70.86</b>	<b>63.91</b>	69.70	70.50	68.14
	CombNorm	80.00	55.64	21.44	68.59	18.90	18.53	78.11	40.93	40.90	<b>70.71</b>	<b>71.77</b>	<b>69.91</b>
	NoNorm	82.43	21.78	21.21	<b>71.40</b>	19.78	19.85	79.75	39.18	39.00	69.45	67.99	46.38
SGC	BatchNorm	79.32	15.86	14.40	61.60	17.34	17.82	76.34	54.22	29.49	<b>68.58</b>	65.54	62.33
	PairNorm	80.78	71.26	51.03	69.76	60.14	50.94	75.81	68.89	62.14	60.72	39.69	26.67
	NodeNorm	78.09	<b>78.77</b>	73.93	63.42	61.81	60.22	71.64	71.50	73.30	63.21	26.81	16.18
	MeanNorm	80.22	48.29	30.07	70.78	38.27	28.27	75.07	47.29	41.32	54.86	21.74	18.97
	GroupNorm	<b>82.81</b>	75.81	<b>74.94</b>	72.32	67.54	61.75	<b>78.87</b>	<b>76.43</b>	<b>74.62</b>	66.12	<b>67.29</b>	<b>66.11</b>
	CombNorm	77.65	75.16	74.45	63.66	59.97	54.52	71.67	71.50	72.23	65.73	54.37	47.52
	NoNorm	79.38	75.93	68.75	<b>72.36</b>	<b>71.06</b>	<b>62.64</b>	78.01	69.06	66.55	61.96	41.43	34.24

★ *NodeNorm*. [37]

$$\text{NodeNorm}(\mathbf{x}_i; p) = \frac{\mathbf{x}_i}{\text{std}(\mathbf{x}_i)^{\frac{1}{p}}}.$$

★ *MeanNorm*. [41]

$$\text{MeanNorm}(\mathbf{x}_{(k)}) = \mathbf{x}_{(k)} - \mathbb{E}[\mathbf{x}_{(k)}].$$

★ *BatchNorm*. [38]

$$\text{BatchNorm}(\mathbf{x}_{(k)}) = \gamma \cdot \frac{\mathbf{x}_{(k)} - \mathbb{E}[\mathbf{x}_{(k)}]}{\text{std}(\mathbf{x}_{(k)})} + \beta.$$

★ *GroupNorm*. [42]

$$\text{GroupNorm}(\mathbf{X}; G, \lambda) = \mathbf{X} + \lambda \cdot \sum_{g=1}^G \text{BN}(\tilde{\mathbf{X}}_g), \tilde{\mathbf{X}}_g = \text{softmax}(\mathbf{X} \cdot \mathbf{U})[:, g] \circ \mathbf{X}.$$

Here  $s$  in *PairNorm* is a hyperparameter controlling the average pair-wise variance and we choose  $s = 1$  in our case.  $p$  in *NodeNorm* denotes the normalization order and our paper uses  $p = 2$ .  $\text{std}(\cdot)$  and  $\mathbb{E}[\cdot]$  are functions that calculate the standard deviation and mean value, respectively.  $\circ$  in *GroupNorm* is the operation of a row-wise multiplication,  $\mathbf{U} \in \mathbb{R}^{d \times G}$  represents a learned transformation,  $G$  means the number of groups, and  $\lambda$  is the skip connection coefficient used in *GroupNorm*. Specifically, in our implementation, we adopt  $(G, \lambda) = (10, 0.03)$  for Cora,  $(5, 0.01)$  for Pubmed, and  $(10, 0.005)$  for Citeceer and OGBN-ArXiv. *CombNorm* normalizes layer-wise graph embeddings by successively applying the two top-performing *GroupNorm* and *NodeNorm*.

**Experimental observations.** Extensive results are collected in Table 4 and 17. We conclude in the following: (i) *Dataset dependent observations.* On small datasets such as Cora and Citeseer, non-parametric normalization methods such as NodeNorm and PairNorm often present on-par performance with parametric GroupNorm, and GroupNorm displays better performance than CombNorm (i.e., GroupNorm + NodeNorm). On the contrary for large graphs such as OGBN-ArXiv, GroupNorm and CombNorm show a superior generalization ability than non-parametric normalizations, and adding NodeNorm on top of GroupNorm leads to extra improvements on deep GCN backbones. (ii) *Backbone dependent observations.* We observe that even the same normalization technique usually appears diverse behaviors on different GNN backbones. For example, PairNorm is nearly always better than NodeNorm on 16 and 32 layers of GCN on three small datasets, and worse than NodeNorm on OGBN-ArXiv. However the case is almost reversed when

we experiment with the SGC backbone, where NodeNorm is outperforming PairNorm on small graphs and inferior on OGBN-ArXiv, for 16/32 layers GNNs. Meanwhile, we notice that SGC with normalization tricks achieve similar performance to GCN backbone on three small graphs, while consistently fall behind on large-scale OGBN graphs. (iii) *Stability observations.* In general, training deep GNNs with normalization incurs more instability (e.g., large performance variance) along with the increasing depth of GNNs. BatchNorm demonstrates degraded performance with large variance on small graphs, and yet it is one of the most effective mechanism on the large graph with outstanding generalization and improved stability. (iv) Overall, across the five investigated norms, GroupNorm has witnessed most of top-performing scenarios, and PairNorm/NodeNorm occupied second best performance in GCN/SGC respectively, dependent on the scale of datasets. In contrast, MeanNorm performs the worst in training deep GCN/SGC, in terms of both achievable accuracy and performance stability.

### 3.4 Random Dropping

**Formulations.** Random dropping [34], [35], [78], [88] is another group of approaches to address the over-smoothing issue by randomly removing or sampling a certain number of edges or nodes at each training epoch. Theoretically, it is effective in decelerating the over-smoothing and relieving the information loss caused by dimension collapse [34], [35].

As described above,  $\mathbf{X}^l \in \mathbb{R}^{n \times d}$  is the node embeddings at the  $l$ -th layer. Let  $\mathfrak{R}(\mathbf{A}) = (\mathbf{I} + \mathbf{D})^{-1/2}(\mathbf{I} + \mathbf{A})(\mathbf{I} + \mathbf{D})^{-1/2}$  denotes a normalization operator, where  $\mathbf{A} \in \mathbb{R}^{n \times n}$  is the adjacency matrix. Then, a vanilla GCN layer can be written as  $\mathbf{X}^{l+1} = \mathfrak{R}(\mathbf{A})\mathbf{X}^l\mathbf{W}^l$ , where  $\mathbf{W}^l \in \mathbb{R}^{d \times d}$  denotes the weight matrix of the  $l$ -th layer.

★ *Dropout*. [78]  $\mathbf{X}^{l+1} = \mathfrak{R}(\mathbf{A})(\mathbf{X}^l \odot \mathbf{Z}^l)\mathbf{W}^l$ , where  $\mathbf{Z}^l \in \{0, 1\}^{n \times d}$  is a binary random matrix, and each element  $Z_{ij}^l \sim \text{Bernoulli}(\pi)$  is drawn from Bernoulli distribution.

★ *DropEdge*. [34]  $\mathbf{X}^{l+1} = \mathfrak{R}(\mathbf{A} \odot \mathbf{Z}^l)\mathbf{X}^l\mathbf{W}^l$ , where  $\mathbf{Z}^l \in \{0, 1\}^{n \times n}$  is a binary random matrix, and each element  $Z_{ij}^l \sim \text{Bernoulli}(\pi)$  is drawn from Bernoulli distribution.

★ *DropNode*. [35]  $\mathbf{X}^{l+1} = \mathfrak{R}(\mathbf{Q}^{l+1}\mathbf{A} \text{diag}(\mathbf{Z}^l)\mathbf{Q}^{l\top})\mathbf{X}^l\mathbf{W}^l$ , where  $\mathbf{Z}^l \in \{0, 1\}^n$  is a binary random matrix, and each

TABLE 5

Test accuracy (%) under different random dropping. Experiments are conducted on Cora, Citeseer, PubMed, and OGBN-ArXiv with 2/16/32 layers GCN and SGC. Performance are averaged from 100 repetitions, and standard deviations are reported in Table 18, 19, 20. Dropout rates are tuned for best performance.

Dataset	Settings	Cora			Citeseer			PubMed			OGBN-ArXiv		
		2	16	32	2	16	32	2	16	32	2	16	32
GCN	No Dropout	80.68	<b>28.56</b>	<b>29.36</b>	71.36	23.19	<b>23.03</b>	79.56	39.85	40.00	<b>69.53</b>	66.14	41.96
	Dropout	<b>82.39</b>	21.60	21.17	<b>71.43</b>	19.37	20.15	<b>79.79</b>	39.09	39.17	69.40	67.79	45.41
	DropNode	77.10	27.61	27.65	69.38	21.83	22.18	77.39	40.31	40.38	66.67	67.17	43.81
	DropEdge	79.16	28.00	27.87	70.26	22.92	22.92	78.58	40.61	40.50	68.67	66.50	<b>51.70</b>
	LADIES	77.12	28.07	27.54	68.87	22.52	22.60	78.31	40.07	40.11	66.43	62.05	40.41
	DropNode+Dropout	81.02	22.24	18.81	70.59	24.49	18.23	78.85	40.44	40.37	68.66	68.27	44.18
	DropEdge+Dropout	79.71	20.45	21.10	69.64	19.77	18.49	77.77	40.71	40.51	66.55	<b>68.81</b>	49.82
	LADIES+Dropout	78.88	19.49	16.92	69.02	<b>27.17</b>	18.54	78.53	<b>41.43</b>	<b>40.70</b>	66.35	65.13	39.99
SGC	No Dropout	77.55	73.99	66.80	71.80	<b>72.69</b>	70.50	77.59	69.74	67.81	<b>62.34</b>	<b>42.54</b>	<b>34.76</b>
	Dropout	79.37	75.91	68.40	<b>72.35</b>	71.21	62.35	78.04	69.12	66.53	61.96	41.47	34.22
	DropNode	78.57	76.99	<b>72.93</b>	71.87	72.50	<b>70.60</b>	77.63	72.51	68.16	61.21	40.52	34.64
	DropEdge	78.68	70.65	44.00	71.94	69.43	45.13	<b>78.26</b>	68.39	52.08	62.06	41.03	33.61
	LADIES	78.50	<b>78.35</b>	72.71	71.88	71.69	69.80	77.65	<b>74.86</b>	<b>72.27</b>	61.49	38.96	33.17
	DropNode+Dropout	<b>80.60</b>	74.83	55.04	72.33	70.30	65.85	78.10	67.98	52.01	61.54	39.48	32.63
	DropEdge+Dropout	80.27	76.19	66.08	72.09	66.48	35.55	77.63	69.65	67.55	60.21	39.12	33.81
	LADIES+Dropout	79.81	74.72	66.62	71.85	69.24	50.81	77.46	70.54	67.94	60.27	31.41	24.86

element  $\mathbf{Z}_j^l \sim \text{Bernoulli}(\pi)$  is drawn from Bernoulli distribution. Suppose the index of selected nodes are  $i_1, i_2, \dots, i_{s_l}$ ,  $\mathbf{Q}^l \in \{0, 1\}^{s_l \times n}$  is a row selection matrix, where  $\mathbf{Q}_{k,m}^l = 1$  if and only if the  $m = i_k$ , and  $1 \leq k \leq s_l, 1 \leq m \leq n$ .

★ LADIES. [88]  $\mathbf{X}^{l+1} = \Re(\mathbf{Q}^{l+1} \mathbf{A} \text{diag}(\mathbf{Z}^l) \mathbf{Q}^{l\top}) \mathbf{X}^l \mathbf{W}^l$ , where  $\mathbf{Z}^l \in \{0, 1\}^n$  is a binary random matrix with  $\|\mathbf{Z}^l\|_0 = s_l$ , and each element  $\mathbf{Z}_j^l \sim \text{Bernoulli}\left(\frac{\|\mathbf{Q}^l \mathbf{A}_{:,j}\|_2^2}{\|\mathbf{Q}^l \mathbf{A}\|_F^2}\right)$  is drawn from Bernoulli distribution.  $\mathbf{Q}^l \in \{0, 1\}^{s_l \times n}$  is the row selection matrix sharing the same definition in *DropNode*.

For these dropout techniques, the neuron dropout rate follows the “sweet point” configuration in Table 2, and the graph dropout rates are picked from  $\{0.2, 0.5, 0.7\}$  to attain best results. All presented results adopt the layer-wise dropout scheme consistent with the one in [76].

**Experimental observations.** Main evaluation results of random dropping mechanisms are presented in Table 5 and 18, and additional results are referred to Table 19 and 20. Several interesting findings can be summarized as follows: (i) The overall performance of random dropping is not as significant as skip connection and graph normalization. Such random dropping tricks at most retard the performance drop, but can not boost deep GNNs to be stronger than shallow GNNs. For examples, on Cora dataset, all dropouts fail to improve deep GCNs; on OGBN-ArXiv dataset, all dropouts also fail to benefits deep SGCs. On other graph datasets, only a small subset of dropping approaches can relieve performance degradation, while others tricks still suffer accuracy deterioration. (ii) The effects of random dropping vary drastically across models, datasets, and layer numbers. It is hard to find a consistently improving technique. To be specific, we observe that, *Sensitive to models*: DropNode on SGC has been shown as an effective training trick for Cora dataset, but turns out to be useless when cooperating with GCN; *Sensitive to datasets*: On Pubmed dataset, the LADIES is the best trick, while it becomes the worst one on OGBN-ArXiv; *Sensitive to layer number*: Deepening SGC from 16 layers to 32 layers, the performance of DropEdge declines significantly from 65% ~ 70% to 40% ~ 50%. A noteworthy exception is LADIES trick on PubMed, which

consistently achieves the best result for both 16/32-layer GCN and SGC. (iii) Dropout (with common rate setting 0.6) is demonstrated to be beneficial and stronger than node or edge dropping for shallow GCNs (i.e., 2 layers). However, this dropout rate downgrades the performance when GCN goes deeper. Combining Dropout with graph dropping may not always be helpful. For instance, incorporating dropout into LADIES downgrades the accuracy of 32 layers SGC from 69.8% to 50.8%. (iv) SGC with random dropping shows better tolerance for deep architectures, and more techniques presented in Table 5 can improve the generalization ability compared to the plain GCN. Meanwhile, with the same random dropping, SGC steadily surpasses GCN by a substantial performance margin for training deep GNN (e.g.,  $\geq 16$  layers) on three small graph datasets, while GCN shows a superior accuracy on large-scale OGBN graphs. (v) From the stability perspective, we notice that SGC consistently has smaller performance variance than GCN of which instability is significantly enlarged by the increasing depth.

TABLE 6

Average test accuracy (%) and its standard deviations from 100 independent repetitions w. or w.o. the identity mapping.

Dataset	Identity Mapping	GCNs		
		2	16	32
Cora	with	<b>82.98±0.75</b>	<b>67.23±3.61</b>	<b>40.57±11.7</b>
	without	82.38±0.33	21.49±3.84	21.22±3.71
Citeseer	with	68.25±0.71	<b>56.39±4.36</b>	<b>35.28±5.85</b>
	without	<b>71.46±0.44</b>	19.59±1.96	20.29±1.79
PubMed	with	79.09±0.48	<b>79.55±0.41</b>	<b>73.74±0.71</b>
	without	<b>79.76±0.39</b>	39.14±1.38	38.77±1.20
OGBN-ArXiv	with	<b>71.08±0.28</b>	<b>69.22±0.84</b>	<b>62.85±2.22</b>
	without	69.46±0.22	67.96±0.38	45.48±4.50

### 3.5 Other Tricks

Although there are multiple other tricks in literature, such as shallow sub-graph sampling [86] and geometric scattering transform of adjacency matrix [75], most of them are intractable to be incorporated into the existing deep GNN frameworks. To be specific, the shallow sub-graph sampling has to sample the shallow neighborhood for each node

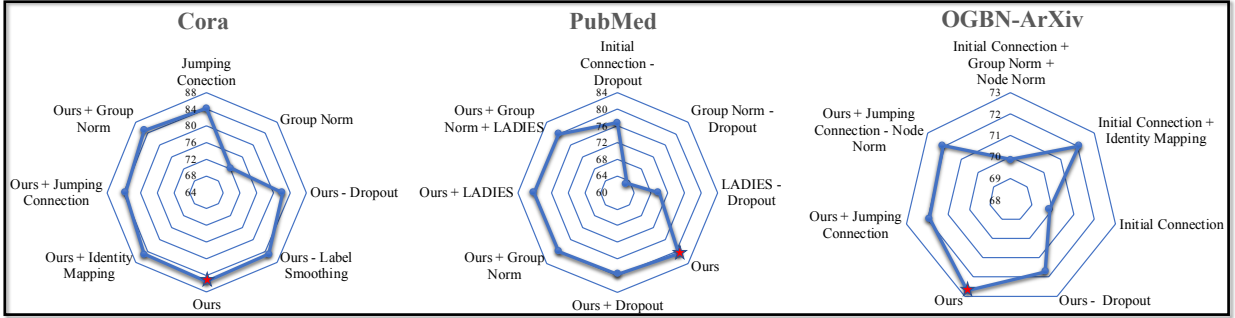


Fig. 2. Average test accuracy (%) from 100 independent repetitions on Cora, PubMed, and OGBN-ArXiv graphs respectively. *Ours* indicates our best combo of tricks on the corresponding dataset.  $-/+$  means add/remove certain tricks from the trick combos. The top-performing setups are highlighted with red points.

TABLE 7

Test accuracy (%) comparison with other previous state-of-the-art frameworks. Experiments are conducted on Cora, Citeseer, PubMed, and OGBN-ArXiv with 2/16/32 GNNs. Performance are averaged from 100 repetitions, and standard deviations are reported in Table 21. The superior performance achieved by **our best tricks combo** with deep GCNs (i.e.,  $\geq 16$  layers) are highlighted in the first row.

Model	Cora ( <b>Ours: 85.48</b> )			Citeseer ( <b>Ours: 73.35</b> )			PubMed ( <b>Ours: 80.76</b> )			ArXiv ( <b>Ours: 72.70</b> )		
	2	16	32	2	16	32	2	16	32	2	16	32
SGC [83]	79.31	75.98	68.45	72.31	71.03	61.92	78.06	69.18	66.61	61.98	41.58	34.22
DAGNN [33]	80.30	84.14	83.39	18.22	73.05	72.59	77.74	80.32	80.58	67.65	71.82	71.46
GCNII [29]	82.19	84.69	85.29	67.81	72.97	73.24	78.05	80.03	79.91	71.24	72.61	72.60
JKNet [32]	79.06	72.97	73.23	66.98	54.33	50.68	77.24	64.37	63.77	63.73	66.41	66.31
APNP [30]	82.06	83.64	83.68	71.67	72.13	72.13	79.46	80.30	80.24	65.31	66.95	66.94
GPRGNN [89]	82.53	83.69	83.13	70.49	71.39	71.01	78.73	78.78	78.46	69.31	70.30	70.18

iteratively and the geometric scattering requires multiscale wavelet transforms on matrix  $\mathbf{A}$ . Both of them do not directly propagate message based upon  $\mathbf{A}$ , which is deviate from the common fashion of deep GNNs. Fortunately, we find that the *Identity Mapping* proposed in [29] is effective to augment existing frameworks and relieves the over-smoothing and overfitting issues. It can be depicted as follows:

★ *Identity Mapping*. [29]  $\mathbf{X}^{l+1} = \sigma(\mathbf{A}\mathbf{X}^l(\beta_l \cdot \mathbf{W}^l + (1 - \beta_l) \cdot \mathbf{I}))$ ,  $\beta_l$  is computed by  $\beta_l = \log(\frac{\lambda}{l} + 1)$ , where  $\lambda$  is a positive hyperparameter, and  $\beta_l$  decreases with layers to avoid the overfitting. In our case,  $\lambda$  is grid searched for different graph datasets:  $\lambda = 0.1$  for Cora, Citeseer and PubMed, and  $\lambda = 0.5$  for OGBN-ArXiv.

**Experimental observations.** As shown in Table 6, we conduct experiments on 2/16/32 layers GCNs with or without the identity mapping. From the results on {Cora, Citeseer, PubMed, OGBN-ArXiv} datasets, (i) we find the identity mapping consistently brings deep GCNs (e.g., 16/32 layers) significant accuracy improvements up to {45.74%, 36.80%, 40.41%, 17.37%}, respectively. It empirically evidenced the effectiveness of identity mapping technique in mitigating over-smoothing issue, particularly for small graphs. However, on shallow GCNs (e.g., 2 layers), identity mapping does not work very well, which either obtains a marginal gain or even incurs some degradation. (ii) Although the generalization for deep GCNs on small-scale graphs (e.g., Cora and Citeseer) is largely enhanced, it also amplify the performance instability.

#### 4 BEST COMBO OF INDIVIDUAL TRICKS

In the last section, we evaluate the different training tricks of each category fairly with *ceteris paribus*. However, being augmented with one specific trick, it is observed that deep GNNs often perform worse than their shallow variants since

they are **NOT trained well** to fully tackle the issues of over-smoothing, overfitting and gradient vanishing. Considering the standard training of other deep neural networks (e.g., CNNs [72] mixed with skip connection, normalization, dropout, learning rate decay, etc.), it is unpractical to stack deep GNNs with a standalone trick to get the desired performance. Based on the benchmark analysis, we are thus motivated to summarize the powerful trick combos and shed novel insight into the design philosophy of deep graph neural networks.

**The best trick combos:** Provided that the “sweet point” hyperparameter configurations in Table 2 are adopted: ❶ On Cora, 64 layers SGC with *Initial Connection*, *Dropout*, and *Label Smoothing*; ❷ On PubMed, 32 layers SGC with *Jumping Connection* and *No Dropout*; ❸ On Citeseer, 32 layers GCN with *Initial Connections*, *Identity Mapping*, and *Label Smoothing*; ❹ On OGBN-ArXiv, 16 layer GCNII with *Initial Connection*, *Identity Mapping*, *GroupNorm*, *NodeNorm*, and *Dropout*.

#### 4.1 Our best combos of tricks and ablation study

We summarize our best trick combos for Cora, Citeseer, PubMed, and OGBN-ArXiv in the above box. Meanwhile, comprehensive ablation studies are conducted to support the superiority of our trick combos in Figure 2. For each dataset, we examine 7 ~ 8 combination variants by adding, removing or replacing certain tricks from our best trick combo. Results extensively endorse our carefully selected combinations.

#### 4.2 Comparison to state-of-the-art frameworks.

To further validate the effectiveness of our explored best combos, we perform comparisons with other previous state-of-the-art frameworks, including SGC [83], DAGNN [33],

TABLE 8

Transfer studies of our trick combos based on SGC (*Ours*). Comparison are conducted on eight hold out datasets with two widely adopted baselines, i.e., GCNII and DAGNN. Performance are averaged from 100 independent runs. All GNNs have 32 layers.

Category	CS	Physics	Computers	Photo	Texas	Wisconsin	Cornell	Actor
SGC	70.52±3.96	91.46±0.48	37.53±0.20	26.60±4.64	56.41±4.25	51.29±6.44	58.57±3.44	26.17±1.15
DAGNN	89.60±0.71	93.31±0.60	<b>79.73±3.63</b>	89.96±1.16	57.68±5.07	50.84±6.62	58.43±3.93	27.73±1.08
GCNII	71.67±2.68	93.15±0.92	37.56±0.43	62.95±9.41	69.19±6.56	70.31±4.75	74.16±6.48	34.28±1.12
JKNet	81.82±3.32	90.92±1.61	67.99±5.07	78.42±6.95	61.08±6.23	52.76±5.69	57.30±4.95	28.80±0.97
APNP	<b>91.61±0.49</b>	93.75±0.61	43.02±10.16	59.62±23.27	60.68±4.50	54.24±5.94	58.43±3.74	28.65±1.28
GPRGNN	89.56±0.47	93.49±0.59	41.94±9.95	<b>91.74±0.81</b>	62.27±4.97	71.35±5.56	58.27±3.96	29.88±1.82
DGMLP [84]	88.13±1.06	92.07±0.31	37.4±0.00	25.31±0.00	64.86±0.00	52.94±0.0	54.05±0.00	25.45±0.15
Ours on SGC	90.74±0.66	<b>94.12±0.56</b>	75.40±1.88	88.29±1.73	<b>79.68±3.77</b>	<b>83.59±3.32</b>	<b>81.24±5.77</b>	<b>36.84±0.70</b>

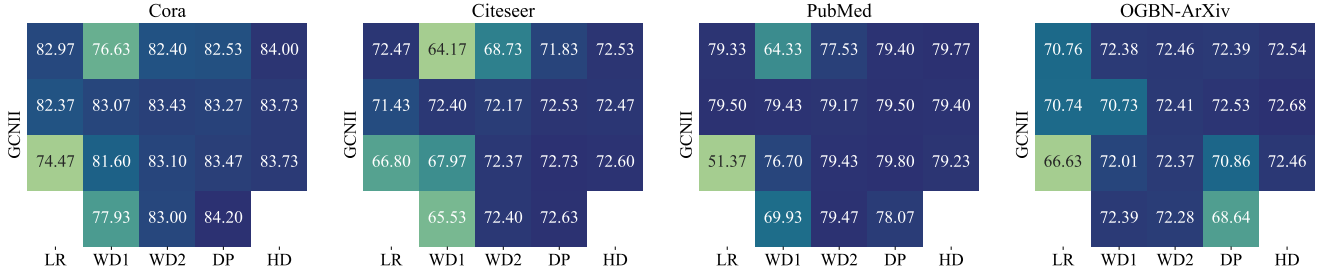


Fig. 3. The hyperparameter investigation of GCNII on Cora, Citeseer, Pubmed, and OGBN-ArXiv. Node classification accuracies are presented in a manner of heatmap. From top to bottom, learning rate (LR), weight decay for the hidden layers (WD 1), weight decay for the prediction layer (WD 2), dropout (DP), and hidden dimension (HD) traverse from left to right in  $\{0.01, 0.001, 0.0001\}$ ,  $\{0, 0.01, 0.001, 0.0001\}$ ,  $\{0, 1 \times 10^{-4}, 2 \times 10^{-4}, 5 \times 10^{-4}\}$ ,  $\{0.1, 0.2, 0.5, 0.7\}$ , and  $\{128, 256, 512\}$ , respectively.

TABLE 9

Training time per epoch (ms) and the max allocated memory (MB) for skip connection tricks.

Backbone	Settings	Cora						Citeseer					
		2		16		32		2		16		32	
		Time	Memory	Time	Memory	Time	Memory	Time	Memory	Time	Memory	Time	Memory
GCN	None	3.09	191.92	20.12	196.35	30.36	201.40	5.49	511.80	20.54	529.13	33.99	548.94
	Residual	6.03	43.32	23.56	77.83	36.78	117.26	6.07	161.10	24.81	326.90	39.71	515.66
	Initial	6.13	43.32	23.11	77.83	36.22	117.26	6.39	161.10	25.11	325.27	36.48	514.03
	Jumping	5.37	43.32	22.13	84.96	32.32	134.45	5.40	161.11	24.25	365.55	35.18	606.49
	Dense	6.94	44.80	32.39	180.97	40.78	502.90	7.17	168.84	33.11	895.55	97.50	2623.16
SGC	None	4.23	42.56	10.95	67.16	19.24	95.27	3.96	156.99	10.99	265.31	18.12	390.08
	Residual	4.66	42.56	16.04	67.16	23.06	95.27	4.44	155.09	15.43	264.26	23.49	389.04
	Initial	4.53	42.56	15.05	67.16	23.19	95.27	4.88	156.99	16.19	264.26	23.51	389.04
	Jumping	4.06	42.57	13.14	73.63	20.40	111.80	3.96	157.00	13.61	301.56	20.30	478.52
	Dense	5.77	44.04	25.61	169.64	39.11	480.24	5.88	164.09	30.31	830.34	89.48	2493.59
GCN	None	8.36	535.83	64.80	1298.71	130.28	2350.06	133.14	5856.61	1136.12	14058.69	2295.50	23432.50
	Residual	11.99	445.36	76.30	1365.64	150.39	2415.98	162.19	6399.08	1226.54	14601.16	2447.16	23974.96
	Initial	12.08	445.36	76.30	1365.64	150.21	2415.98	162.42	6399.08	1227.36	14601.16	2459.27	23974.96
	Jumping	12.29	445.36	74.00	1525.13	145.12	2883.86	160.46	6399.15	1209.07	14602.33	2433.02	24979.94
	Dense	15.07	486.37	186.55	4240.60	575.00	13360.93	186.89	6732.33	2202.83	37004.45	4001.04	117163.48
SGC	None	8.99	424.60	49.02	1066.66	95.34	1800.10	135.20	6232.20	1004.12	12109.80	2014.96	18826.87
	Residual	10.10	424.60	57.31	1066.66	111.84	1796.37	144.02	6232.20	1073.04	12108.55	2137.83	18824.99
	Initial	9.88	424.60	57.29	1066.66	111.81	1796.37	143.88	6232.20	1074.09	12108.55	2149.85	18824.99
	Jumping	9.29	424.61	54.86	1207.24	106.82	2248.57	142.14	6232.28	1058.32	12110.97	2125.41	19666.49
	Dense	12.68	465.62	166.10	3917.57	531.66	12721.31	168.23	6565.46	2037.07	34512.94	1935.8	53336.16

GCNII [29], JKNet [32], APPNP [30], GPRGNN [89]. As shown in Table 7, we find that organically combining the existing training tricks consistently outperforms the previous elaborately crafted deep GCNs frameworks, on both small- and large-scale graph datasets.

### 4.3 Transferring trick combos across datasets.

The last sanity check is whether there exist certain trick combos can be effective across multiple different graph datasets. Therefore, we pick *Initial Connection + GroupNorm* as the trick combo since these two techniques achieve optimal performance under most of scenarios in Section 3.2, 3.3, and 3.4, and this trick combo also performs on-par with

the best trick combo on Cora and OGBN-ArXiv. Specially, we evaluate it on **eight** other open-source graph datasets: (i) two Co-author datasets [90] (CS and Physics), (ii) two Amazon datasets [90] (Computers and Photo), (iii) three WebKB datasets [91] (Texas, Wisconsin, Cornell), and (iv) the Actor dataset [91]. In these transfer investigations, we follow the exact “sweet point” settings from Cora in Table 2, except that for two Coauthor datasets, the weight decay is set to 0 and the dropout rate is set to 0.8, and in two Amazon datasets the dropout rate is set to 0.5, as adopted by [33].

As shown in Table 8, (i) our chosen trick combo (i.e., *Initial Connection + GroupNorm*) **universally encourages the worst-**

TABLE 10  
Training time per epoch (ms) and the max allocated memory (MB) for normalization tricks.

Backbone	Settings	Cora						Citeseer					
		2		16		32		2		16		32	
		Time	Memory	Time	Memory	Time	Memory	Time	Memory	Time	Memory	Time	Memory
GCN	None	3.09	191.92	20.12	196.35	30.36	201.40	5.49	511.80	20.54	529.13	33.99	548.94
	BatchNorm	3.57	191.93	23.15	196.40	35.97	201.51	5.84	511.81	24.58	529.23	38.17	606.99
	PairNorm	5.90	191.92	35.19	196.35	41.79	201.40	6.76	511.80	36.61	529.13	42.99	607.39
	NodeNorm	5.26	191.92	32.45	196.35	41.91	201.40	6.57	511.80	33.79	529.13	38.97	707.63
	MeanNorm	3.82	191.92	25.56	196.35	38.25	201.40	5.97	511.80	26.53	529.13	37.82	548.94
	GroupNorm	12.92	191.95	40.62	196.67	59.52	348.51	13.20	511.89	40.27	858.86	78.45	1625.21
	CombNorm	14.46	191.95	46.57	208.48	68.62	389.83	14.24	511.89	44.06	958.53	86.17	1827.35
SGC	None	4.23	42.56	10.95	67.16	19.24	95.27	3.96	156.99	10.99	265.31	18.12	390.08
	BatchNorm	4.45	43.23	17.78	77.15	26.09	115.91	5.05	160.26	17.80	315.04	28.38	491.93
	PairNorm	7.28	43.23	28.32	77.08	38.63	115.78	7.29	160.24	28.76	314.05	39.59	491.83
	NodeNorm	6.64	43.90	24.37	87.15	40.00	136.59	6.81	163.50	25.29	363.83	39.92	592.77
	MeanNorm	4.99	42.56	18.28	67.16	29.72	95.27	4.78	156.99	19.04	266.17	27.62	390.94
	GroupNorm	13.76	62.60	43.64	187.56	53.86	336.75	14.80	260.03	41.11	848.65	69.82	1550.90
	CombNorm	15.04	63.94	41.08	207.56	57.30	378.08	15.76	266.54	40.26	946.32	78.38	1752.74
Backbone	Settings	PubMed						OGBN-ArXiv					
		2		16		32		2		16		32	
GCN	None	8.36	535.83	64.80	1298.71	130.28	2350.06	133.14	5856.61	1136.12	14058.69	2295.50	23432.50
	BatchNorm	8.49	535.84	70.19	1586.98	141.15	2945.82	135.88	6022.00	1178.30	16539.43	2378.49	28559.35
	PairNorm	10.08	535.83	87.70	1589.46	176.94	2951.15	146.77	6021.99	1317.47	16539.93	2657.19	28560.36
	NodeNorm	9.80	535.83	85.75	1876.81	173.00	3544.90	146.87	6188.01	1303.23	19029.60	2631.94	33706.34
	MeanNorm	8.70	535.83	72.47	1298.71	145.90	2350.88	137.85	5856.61	1191.41	14059.32	2407.81	23433.75
	GroupNorm	14.55	535.88	141.71	3043.47	286.61	5955.95	231.48	7689.02	2388.49	41540.97	4801.72	84847.76
	CombNorm	16.92	535.88	162.72	3623.99	330.01	7156.31	245.18	8020.42	2444.32	43978.73	5204.64	95168.28
SGC	None	8.99	424.60	49.02	1066.76	95.34	1800.10	135.20	6232.20	1004.12	12109.80	2014.96	18826.87
	BatchNorm	9.40	443.88	54.32	1358.60	105.91	2400.34	140.39	6397.60	1045.01	14589.29	2085.69	23951.86
	PairNorm	11.72	443.86	72.73	1358.47	142.71	2400.09	158.84	6397.58	1188.22	14589.16	2377.52	23951.60
	NodeNorm	11.49	463.19	70.80	1645.54	138.86	2996.44	157.50	6563.60	1181.12	17080.08	2354.95	29098.83
	MeanNorm	9.97	424.60	56.75	1066.76	110.74	1800.10	142.81	6232.20	1061.17	12109.80	2127.01	18826.87
	GroupNorm	18.86	578.84	129.27	2814.14	255.70	5412.07	299.06	8064.47	2321.44	39592.63	2334.56	37129.89
	CombNorm	21.56	618.91	150.92	3387.71	299.14	6597.04	321.34	8395.86	1270.12	21882.53	2512.72	42276.51

TABLE 11  
Training time per epoch (ms) and the max allocated memory (MB) for dropout tricks.

Backbone	Settings	Cora						Citeseer					
		2		16		32		2		16		32	
		Time	Memory	Time	Memory	Time	Memory	Time	Memory	Time	Memory	Time	Memory
GCN	None	3.09	191.92	20.12	196.35	30.36	201.40	5.49	511.80	20.54	529.13	33.99	548.94
	DropEdge	3.79	170.99	20.24	174.85	40.34	179.28	6.09	461.56	22.62	478.41	40.66	505.25
	DropNode	3.43	154.91	18.91	158.51	34.31	162.36	5.71	427.82	22.91	448.28	39.12	498.90
	FastGCN	3.68	168.32	19.53	172.38	36.08	176.61	6.15	463.89	22.79	480.76	40.29	504.10
	LADIES	5.60	168.54	29.28	172.60	55.82	179.19	7.24	463.91	34.28	480.76	61.26	504.09
SGC	None	4.23	42.56	10.95	67.16	19.24	95.27	3.96	156.99	10.99	265.31	18.12	390.08
	DropEdge	4.36	41.65	13.97	65.69	26.89	93.18	4.78	151.84	15.07	263.68	28.51	390.11
	DropNode	3.30	40.94	14.77	64.53	25.77	91.64	4.56	149.14	17.08	257.70	29.29	381.35
	FastGCN	3.63	41.60	14.67	65.61	26.71	93.12	4.71	151.82	17.61	263.56	31.78	390.04
	LADIES	5.73	41.61	26.12	65.61	48.57	93.07	5.68	151.80	28.34	264.21	52.29	390.40
Backbone	Settings	PubMed						OGBN-ArXiv					
		2		16		32		2		16		32	
GCN	None	8.36	535.83	64.80	1298.71	130.28	2350.06	133.14	5856.61	1136.12	14058.69	2295.50	23432.50
	DropEdge	8.71	471.35	64.95	1264.26	130.22	2312.64	111.98	4963.70	977.04	13044.54	1977.29	22277.59
	DropNode	8.14	418.39	61.52	1231.69	120.77	2270.86	102.11	4267.52	842.81	12272.71	1695.38	21375.29
	FastGCN	9.52	497.76	68.60	1277.93	136.83	2326.76	136.80	5590.19	1108.86	13754.13	2223.08	23082.86
	LADIES	11.59	497.37	95.30	1278.56	192.06	2326.93	158.54	5591.76	1310.97	13753.46	2622.87	23083.57
SGC	None	8.99	424.60	49.02	1066.76	95.34	1800.10	135.20	6232.20	1004.12	12109.80	2014.96	18826.87
	DropEdge	9.04	391.39	49.26	1028.71	94.95	1757.71	116.09	5340.74	850.09	11095.42	1693.23	17672.46
	DropNode	9.03	365.86	45.43	1002.34	86.39	1731.22	106.58	4672.89	713.64	10275.51	1416.19	16794.15
	FastGCN	10.09	407.25	53.28	1043.69	102.09	1772.71	142.55	5966.34	976.45	11803.59	1940.84	18477.01
	LADIES	12.32	407.25	78.93	1043.35	155.52	1772.43	157.47	5966.72	1176.25	11800.70	2345.02	18474.28

performing SGC to become one of the top-performing candidates. It consistently surpasses SGC, DAGNN, GCNII, JKNet, APPNP, GPRGNN, and DGMLP by a substantial accuracy margin up to 61.69% improvements, except for the comparable performances on CS, Computers, and Photo graph datasets. The superior transfer performance of our trick combo suggests that it is capable of serving as a stronger baseline for future deep GNN researches. (ii) Meanwhile,

we observe that equipping our proposed training tricks improves the stability of SGC (i.e., fewer performance variances) on some graph datasets like CS, Photo, Texas, Wisconsin, and Actor, while incurring degraded stability on the rest of the three datasets. (iii) Our trick combo transfers better on small-scale graph datasets such as Photo, Texas, Wisconsin, Cornell, and Actor, compared to other three larger graph datasets like CS, Physics, and Computers.

## 5 EXTRA ANALYSIS

### 5.1 Hyperparameter Analysis

We consider the key hyperparameters of {learning rate, weight decay, dropout rate, and hidden dimension}, and study their impacts on the deep GNN training. Specifically, a 16-layer GCNII is adopted as the backbone architecture since it normally achieves promising performance in deep GNNs literature. As shown in Figure 3, from the results on Cora, Citeseer, Pubmed, and OGBN-Arxiv, we find that: (i) The optimal dropout rate varies across different scales of datasets; (ii) The weight decay for hidden layers plays a crucial role in deep GNNs, especially in the over-parameterized context (e.g., deep GNNs on small-scale dataset like Cora). (iii) It seems that the deep GNNs' performance is not sensitive to the hidden dimension, and changing it from 128 to 512 only has moderated effects. (iv) In general, our identified "sweet point" of hyperparameters achieves superior results, which demonstrates its rationality as a common configuration to benchmark the deep GNN training tricks.

### 5.2 Complexity Analysis

To analyze the time and space complexity in practice, we conduct experiments on 2/16/32 layers for GNNs with different tricks. From the results on Table 9, 10 and 11, we summarize our observations for different types of tricks as follows. All results are measured on a single Quadro RTX 8000, with Linux + cuda driver 11.2 + PyTorch/torch geometric/torch sparse/etc with cuda 11.1.

**Skip connections.** As shown in Table 9, we can draw the following observations: (i) Residual, initial and jumping connections need negligibly additional training time and on-par memory space compared with vanilla GNNs. It is attributed to that only some constant operations and valid extra memory space are required in skip connections, e.g. initial connection only requires to store the embeddings from the first linear layer and perform several times of adding operation in addition. (ii) Dense connection requires approximately twice the training time and memory space of vanilla GCN, which is apparently impractical when dataset and model go larger.

**Normalization.** As shown in Table 10, the observations on normalization tricks are: (i) Graph Neural Networks with activation-based normalization layers (i.e. BatchNorm, NodeNorm and MeanNorm) have on-par time and space complexity with vanilla GNNs. (ii) Parametric normalization layers (i.e. PairNorm, GroupNorm and CombNorm) require more training time and memory space. It is because these normalization layers have more learnable parameters and requires a number of extra inference time to distinguish node embeddings and mitigate the over-smoothing problem.

**Dropout.** As shown in Table 11, we have the following findings: (i) To prune the graph structure with specified strategies, dropout tricks requires a valid period of time for pruning. Such a pruning procedure is performed every training epoch, and thus time consuming. (ii) With sparsified graph structure, dropout tricks moderately reduce the memory consumption.

## 6 CONCLUSION

Deep graph neural networks (GNNs) is a promising field that has so far been a bit held back by finding out "truly" effective

training tricks to alleviate the notorious over-smoothing issue. This work provides a standardized benchmark with fair and consistent experimental configurations to push this field forward. We broadly investigate dozens of existing approaches on tens of representative graphs. Based on extensive results, we identify the combo of most powerful training tricks, and establish new state-of-the-art performance for deep GNNs. We hope them to lay a solid, fair, and practical evaluation foundations by providing strong baselines and superior trick combos for deep GNN research community.

## ACKNOWLEDGEMENTS

X. Hu is in part supported by NSF (#IIS-1750074, #IIS-1900990, #IIS-1849085). Z. Wang is in part supported by US Army Research Office Young Investigator Award W911NF2010240.

## REFERENCES

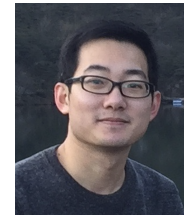
- [1] Y. Li, D. Tarlow, M. Brockschmidt, and R. Zemel, "Gated graph sequence neural networks," *arXiv preprint arXiv:1511.05493*, 2015.
- [2] L. Tang and H. Liu, "Relational learning via latent social dimensions," in *Proceedings of the 15th ACM SIGKDD international conference on Knowledge discovery and data mining*, 2009, pp. 817–826.
- [3] R. Ying, R. He, K. Chen, P. Eksombatchai, W. L. Hamilton, and J. Leskovec, "Graph convolutional neural networks for web-scale recommender systems," in *Proceedings of the 24th ACM SIGKDD International Conference on Knowledge Discovery & Data Mining*, 2018, pp. 974–983.
- [4] K. Zhou, Q. Song, X. Huang, and X. Hu, "Auto-gnn: Neural architecture search of graph neural networks," *arXiv preprint arXiv:1909.03184*, 2019.
- [5] H. Gao, Z. Wang, and S. Ji, "Large-scale learnable graph convolutional networks," in *Proceedings of the 24th ACM SIGKDD International Conference on Knowledge Discovery & Data Mining*, 2018, pp. 1416–1424.
- [6] Y. You, T. Chen, Z. Wang, and Y. Shen, "L2-gcn: Layer-wise and learned efficient training of graph convolutional networks," in *Proceedings of the IEEE/CVF Conference on Computer Vision and Pattern Recognition*, 2020, pp. 2127–2135.
- [7] Y. You, T. Chen, Y. Sui, T. Chen, Z. Wang, and Y. Shen, "Graph contrastive learning with augmentations," *Advances in Neural Information Processing Systems*, vol. 33, 2020.
- [8] Y. You, T. Chen, Z. Wang, and Y. Shen, "Bringing your own view: Graph contrastive learning without prefabricated data augmentations," in *WSDM*. ACM, 2022, p. 1300–1309.
- [9] W. Zheng, E. W. Huang, N. Rao, S. Katariya, Z. Wang, and K. Subbian, "Cold brew: Distilling graph node representations with incomplete or missing neighborhoods," in *International Conference on Learning Representations*, 2022.
- [10] Y. You, T. Chen, Z. Wang, and Y. Shen, "When does self-supervision help graph convolutional networks?" in *Proceedings of the 37th International Conference on Machine Learning*, ser. Proceedings of Machine Learning Research, H. D. III and A. Singh, Eds., vol. 119. PMLR, 13–18 Jul 2020, pp. 10871–10880.
- [11] F. Monti, M. M. Bronstein, and X. Bresson, "Geometric matrix completion with recurrent multi-graph neural networks," *arXiv preprint arXiv:1704.06803*, 2017.
- [12] W. Zheng, E. W. Huang, N. Rao, S. Katariya, Z. Wang, and K. Subbian, "Cold brew: Distilling graph node representations with incomplete or missing neighborhoods," *arXiv:2111.04840*, 2021.
- [13] A. Ortega, P. Frossard, J. Kovačević, J. M. Moura, and P. Vandergheynst, "Graph signal processing: Overview, challenges, and applications," *Proceedings of the IEEE*, vol. 106, 2018.
- [14] T.-K. Hu, F. Gama, T. Chen, W. Zheng, A. Wang, A. R. Ribeiro, and B. M. Sadler, "Scalable perception-action-communication loops with convolutional and graph neural networks," *IEEE Transactions on Signal and Information Processing over Networks*, 2021.
- [15] H. Yang, J. Zhao, W. Zheng, and J. Yu, "Large data throughput optimization model with full c order model parallel flow number prediction optical domain," *TELKOMNIKA (Telecommunication Computing Electronics and Control)*, vol. 14, no. 2A, pp. 10–17, 2016.
- [16] M. Zitnik and J. Leskovec, "Predicting multicellular function through multi-layer tissue networks," *Bioinformatics*, vol. 33, no. 14, pp. i190–i198, 2017.

- [17] N. Wale, I. A. Watson, and G. Karypis, "Comparison of descriptor spaces for chemical compound retrieval and classification," *Knowledge and Information Systems*, vol. 14, no. 3, pp. 347–375, 2008.
- [18] Y. Wang, Y. Sun, Z. Liu, S. E. Sarma, M. M. Bronstein, and J. M. Solomon, "Dynamic graph cnn for learning on point clouds," *Acm Transactions On Graphics (tog)*, vol. 38, no. 5, pp. 1–12, 2019.
- [19] G. Li, M. Muller, A. Thabet, and B. Ghanem, "Deepgcn: Can gcn go as deep as cnns?" in *Proceedings of the IEEE/CVF International Conference on Computer Vision*, 2019, pp. 9267–9276.
- [20] G. Li, M. Müller, G. Qian, I. C. D. Perez, A. Abualshour, A. K. Thabet, and B. Ghanem, "Deepgcn: Can gcn go as deep as cnns," *IEEE Transactions on Pattern Analysis and Machine Intelligence*, 2021.
- [21] K. Duan, Z. Liu, W. Zheng, P. Wang, K. Zhou, T. Chen, Z. Wang, and X. Hu, "Benchmarking large-scale graph training over effectiveness and efficiency," 2018.
- [22] S. Gong, M. Bahri, M. M. Bronstein, and S. Zafeiriou, "Geometrically principled connections in graph neural networks," in *Proceedings of the IEEE/CVF Conference on Computer Vision and Pattern Recognition*, 2020, pp. 11 415–11 424.
- [23] W. Hu, M. Fey, M. Zitnik, Y. Dong, H. Ren, B. Liu, M. Catasta, and J. Leskovec, "Open graph benchmark: Datasets for machine learning on graphs," *arXiv preprint arXiv:2005.00687*, 2020.
- [24] K. Oono and T. Suzuki, "Graph neural networks exponentially lose expressive power for node classification," in *International Conference on Learning Representations*, 2020.
- [25] Q. Li, Z. Han, and X.-M. Wu, "Deeper insights into graph convolutional networks for semi-supervised learning," in *Thirty-Second AAAI Conference on Artificial Intelligence*, 2018.
- [26] H. NT and T. Maehara, "Revisiting graph neural networks: All we have is low-pass filters," *arXiv preprint arXiv:1905.09550*, 2019.
- [27] P. Wang, W. Zheng, T. Chen, and Z. Wang, "Anti-oversmoothing in deep vision transformers via the fourier domain analysis: From theory to practice," *arXiv preprint arXiv:2203.05962*, 2022.
- [28] U. Alon and E. Yahav, "On the bottleneck of graph neural networks and its practical implications," *arXiv preprint arXiv:2006.05205*, 2020.
- [29] M. Chen, Z. Wei, Z. Huang, B. Ding, and Y. Li, "Simple and deep graph convolutional networks," *preprint arXiv:2007.02133*, 2020.
- [30] J. Klicpera, A. Bojchevski, and S. Günnemann, "Predict then propagate: Graph neural networks meet personalized pagerank," *arXiv preprint arXiv:1810.05997*, 2018.
- [31] H. Zhang, T. Yan, Z. Xie, Y. Xia, and Y. Zhang, "Revisiting graph convolutional network on semi-supervised node classification from an optimization perspective," *arXiv preprint arXiv:2009.11469*, 2020.
- [32] K. Xu, C. Li, Y. Tian, T. Sonobe, K.-i. Kawarabayashi, and S. Jegelka, "Representation learning on graphs with jumping knowledge networks," in *International Conference on Machine Learning*. PMLR, 2018, pp. 5453–5462.
- [33] M. Liu, H. Gao, and S. Ji, "Towards deeper graph neural networks," in *Proceedings of the 26th ACM SIGKDD International Conference on Knowledge Discovery & Data Mining*, 2020, pp. 338–348.
- [34] Y. Rong, W. Huang, T. Xu, and J. Huang, "Dropege: Towards deep graph convolutional networks on node classification," in *International Conference on Learning Representations*, 2020.
- [35] W. Huang, Y. Rong, T. Xu, F. Sun, and J. Huang, "Tackling oversmoothing for general graph convolutional networks," *arXiv e-prints*, pp. arXiv–2008, 2020.
- [36] L. Zhao and L. Akoglu, "Pairnorm: Tackling oversmoothing in gnns," *arXiv preprint arXiv:1909.12223*, 2019.
- [37] K. Zhou, Y. Dong, K. Wang, W. S. Lee, B. Hooi, H. Xu, and J. Feng, "Understanding and resolving performance degradation in graph convolutional networks," *arXiv preprint arXiv:2006.07107*, 2020.
- [38] S. Ioffe and C. Szegedy, "Batch normalization: Accelerating deep network training by reducing internal covariate shift," *ICML*, 2015.
- [39] J. L. Ba, J. R. Kiros, and G. E. Hinton, "Layer normalization," *arXiv preprint arXiv:1607.06450*, 2016.
- [40] Y. Wu and K. He, "Group normalization," in *Proceedings of the European Conference on Computer Vision (ECCV)*, 2018, pp. 3–19.
- [41] C. Yang, R. Wang, S. Yao, S. Liu, and T. Abdelzaher, "Revisiting 'over-smoothing' in deep gcn," *preprint arXiv:2003.13663*, 2020.
- [42] K. Zhou, X. Huang, Y. Li, D. Zha, R. Chen, and X. Hu, "Towards deeper graph neural networks with differentiable group normalization," *Advances in Neural Information Processing Systems*, vol. 33, 2020.
- [43] J. Zhou, G. Cui, Z. Zhang, C. Yang, Z. Liu, L. Wang, C. Li, and M. Sun, "Graph neural networks: A review of methods and applications," *arXiv preprint arXiv:1812.08434*, 2018.
- [44] T. N. Kipf and M. Welling, "Semi-supervised classification with graph convolutional networks," *ICLR*, 2017.
- [45] Z. Chen, S. Villar, L. Chen, and J. Bruna, "On the equivalence between graph isomorphism testing and function approximation with gnns," in *Advances in Neural Information Processing Systems*, 2019.
- [46] P. Veličković, G. Cucurull, A. Casanova, A. Romero, P. Lio, and Y. Bengio, "Graph attention networks," *arXiv preprint arXiv:1710.10903*, 2017.
- [47] Z. Ying, J. You, C. Morris, X. Ren, W. Hamilton, and J. Leskovec, "Hierarchical graph representation learning with differentiable pooling," in *NeurIPS*, 2018.
- [48] K. Xu, W. Hu, J. Leskovec, and S. Jegelka, "How powerful are graph neural networks?" *arXiv preprint arXiv:1810.00826*, 2018.
- [49] Y. You, T. Chen, Y. Shen, and Z. Wang, "Graph contrastive learning automated," *arXiv preprint arXiv:2106.07594*, 2021.
- [50] T. Chen, Y. Sui, X. Chen, A. Zhang, and Z. Wang, "A unified lottery ticket hypothesis for graph neural networks," in *Proceedings of the 38th International Conference on Machine Learning*, ser. Proceedings of Machine Learning Research, M. Meila and T. Zhang, Eds., vol. 139. PMLR, 18–24 Jul 2021, pp. 1695–1706.
- [51] T.-K. Hu, F. Gama, T. Chen, Z. Wang, A. Ribeiro, and B. M. Sadler, "Vgai: End-to-end learning of vision-based decentralized controllers for robot swarms," in *ICASSP 2021-2021 IEEE International Conference on Acoustics, Speech and Signal Processing (ICASSP)*. IEEE, 2021, pp. 4900–4904.
- [52] K. Zhou, Q. Song, X. Huang, D. Zha, N. Zou, and X. Hu, "Multi-channel graph neural networks," in *Proceedings of the Twenty-Ninth International Conference on International Joint Conferences on Artificial Intelligence*, 2021, pp. 1352–1358.
- [53] M. Qu, Y. Bengio, and J. Tang, "Gmnn: Graph markov neural networks," *arXiv preprint arXiv:1905.06214*, 2019.
- [54] V. Verma, M. Qu, A. Lamb, Y. Bengio, J. Kannala, and J. Tang, "Graphmix: Regularized training of graph neural networks for semi-supervised learning," *arXiv preprint arXiv:1909.11715*, 2019.
- [55] M. Karimi, D. Wu, Z. Wang, and Y. Shen, "Explainable deep relational networks for predicting compound-protein affinities and contacts," *arXiv preprint arXiv:1912.12553*, 2019.
- [56] V. P. Dwivedi, C. K. Joshi, T. Laurent, Y. Bengio, and X. Bresson, "Benchmarking graph neural networks," *arXiv preprint arXiv:2003.00982*, 2020.
- [57] F. Scarselli, M. Gori, A. C. Tsoi, M. Hagenbuchner, and G. Monfardini, "The graph neural network model," *IEEE Transactions on Neural Networks*, vol. 20, no. 1, pp. 61–80, 2008.
- [58] J. Bruna, W. Zaremba, A. Szlam, and Y. LeCun, "Spectral networks and locally connected networks on graphs," *arXiv*, 2013.
- [59] W. Hamilton, Z. Ying, and J. Leskovec, "Inductive representation learning on large graphs," in *NeurIPS*, 2017, pp. 1024–1034.
- [60] P. Battaglia, R. Pascanu, M. Lai, D. J. Rezende, and K. Kavukcuoglu, "Interaction networks for learning about objects, relations and physics," in *Proceedings of the 30th International Conference on Neural Information Processing Systems*, 2016.
- [61] P. Veličković, G. Cucurull, A. Casanova, A. Romero, P. Liò, and Y. Bengio, "Graph attention networks," in *International Conference on Learning Representations*, 2018.
- [62] K. Xu, W. Hu, J. Leskovec, and S. Jegelka, "How powerful are graph neural networks?" in *International Conference on Learning Representations*, 2019.
- [63] C. Morris, M. Ritzert, M. Fey, W. L. Hamilton, J. E. Lenssen, G. Rattan, and M. Grohe, "Weisfeiler and leman go neural: Higher-order graph neural networks," in *AAAI*, 2019.
- [64] R. Murphy, B. Srinivasan, V. Rao, and B. Ribeiro, "Relational pooling for graph representations," in *International Conference on Machine Learning*, 2019, pp. 4663–4673.
- [65] M. Defferrard, X. Bresson, and P. Vandergheynst, "Convolutional neural networks on graphs with fast localized spectral filtering," in *NeurIPS*, 2016, pp. 3844–3852.
- [66] M. Simonovsky and N. Komodakis, "Dynamic edgeconditioned filters in convolutional neural networks on graphs," in *CVPR*, 2017.
- [67] Y. Wang, J. Jin, W. Zhang, Y. Yu, Z. Zhang, and D. Wipf, "Bag of tricks for node classification with graph neural networks," *arXiv preprint arXiv:2103.13355*, 2021.
- [68] P. Barceló, E. V. Kostylev, M. Monet, J. Pérez, J. Reutter, and J. P. Silva, "The logical expressiveness of graph neural networks," in *International Conference on Learning Representations*, 2020.
- [69] M. K. Matlock, A. Datta, N. Le Dang, K. Jiang, and S. J. Swamidass, "Deep learning long-range information in undirected graphs with

- wave networks," in *2019 International Joint Conference on Neural Networks (IJCNN)*. IEEE, 2019, pp. 1–8.
- [70] K. Zhou, X. Huang, D. Zha, R. Chen, L. Li, S.-H. Choi, and X. Hu, "Dirichlet energy constrained learning for deep graph neural networks," *Advances in Neural Information Processing Systems*, vol. 34, 2021.
- [71] D. Chen, Y. Lin, W. Li, P. Li, J. Zhou, and X. Sun, "Measuring and relieving the over-smoothing problem for graph neural networks from the topological view," in *Proceedings of the AAAI Conference on Artificial Intelligence*, vol. 34, 2020, pp. 3438–3445.
- [72] K. He, X. Zhang, S. Ren, and J. Sun, "Deep residual learning for image recognition," in *CVPR*, 2016, pp. 770–778.
- [73] G. Li, C. Xiong, A. Thabet, and B. Ghanem, "Deepergcn: All you need to train deeper gcn," *arXiv preprint arXiv:2006.07739*, 2020.
- [74] S. Luan, M. Zhao, X.-W. Chang, and D. Precup, "Break the ceiling: Stronger multi-scale deep graph convolutional networks," *arXiv preprint arXiv:1906.02174*, 2019.
- [75] Y. Min, F. Wenkel, and G. Wolf, "Scattering gcn: Overcoming oversmoothness in graph convolutional networks," *arXiv preprint arXiv:2003.08414*, 2020.
- [76] D. Zou, Z. Hu, Y. Wang, S. Jiang, Y. Sun, and Q. Gu, "Layer-dependent importance sampling for training deep and large graph convolutional networks," *NeurIPS*, 2019.
- [77] A. Hasanzadeh, E. Hajiramezani, S. Boluki, M. Zhou, N. Duffield, K. Narayanan, and X. Qian, "Bayesian graph neural networks with adaptive connection sampling," in *International Conference on Machine Learning*. PMLR, 2020, pp. 4094–4104.
- [78] N. Srivastava, G. Hinton, A. Krizhevsky, I. Sutskever, and R. Salakhutdinov, "Dropout: a simple way to prevent neural networks from overfitting," *The journal of machine learning research*, vol. 15, no. 1, pp. 1929–1958, 2014.
- [79] W. Jin, X. Liu, Y. Ma, C. Aggarwal, and J. Tang, "Towards feature overcorrelation in deeper graph neural networks," 2022.
- [80] K. Guo, K. Zhou, X. Hu, Y. Li, Y. Chang, and X. Wang, "Orthogonal graph neural networks," *Proceedings of the AAAI Conference on Artificial Intelligence*, 2022.
- [81] G. Li, M. Müller, B. Ghanem, and V. Koltun, "Training graph neural networks with 1000 layers," in *International conference on machine learning*. PMLR, 2021, pp. 6437–6449.
- [82] L. Zheng, D. Fu, and J. He, "Tackling oversmoothing of gcn with contrastive learning," *arXiv preprint arXiv:2110.13798*, 2021.
- [83] F. Wu, T. Zhang, A. H. d. Souza Jr, C. Fifty, T. Yu, and K. Q. Weinberger, "Simplifying graph convolutional networks," *arXiv preprint arXiv:1902.07153*, 2019.
- [84] W. Zhang, Z. Sheng, Y. Jiang, Y. Xia, J. Gao, Z. Yang, and B. Cui, "Evaluating deep graph neural networks," *arXiv preprint arXiv:2108.00955*, 2021.
- [85] K. Xu, M. Zhang, S. Jegelka, and K. Kawaguchi, "Optimization of graph neural networks: Implicit acceleration by skip connections and more depth," *arXiv preprint arXiv:2105.04550*, 2021.
- [86] H. Zeng, M. Zhang, Y. Xia, A. Srivastava, A. Malevich, R. Kannan, V. Prasanna, L. Jin, and R. Chen, "Deep graph neural networks with shallow subgraph samplers," *preprint arXiv:2012.01380*, 2020.
- [87] M. Fey and J. E. Lenssen, "Fast graph representation learning with PyTorch Geometric," in *ICLR Workshop*, 2019.
- [88] D. Zou, Z. Hu, Y. Wang, S. Jiang, Y. Sun, and Q. Gu, "Layer-dependent importance sampling for training deep and large graph convolutional networks," in *Advances in Neural Information Processing Systems*, H. Wallach, H. Larochelle, A. Beygelzimer, F. d'Alché-Buc, E. Fox, and R. Garnett, Eds., vol. 32. Curran Associates, Inc., 2019.
- [89] E. Chien, J. Peng, P. Li, and O. Milenkovic, "Adaptive universal generalized pagerank graph neural network," in *International Conference on Learning Representations*, 2021.
- [90] O. Shchur, M. Mumme, A. Bojchevski, and S. Günnemann, "Pitfalls of graph neural network evaluation," *arXiv preprint arXiv:1811.05868*, 2018.
- [91] H. Pei, B. Wei, K. C.-C. Chang, Y. Lei, and B. Yang, "Geom-gcn: Geometric graph convolutional networks," in *ICLR*, 2020.
- [92] Y. Shi, Z. Huang, W. Wang, H. Zhong, S. Feng, and Y. Sun, "Masked label prediction: Unified message passing model for semi-supervised classification," *arXiv preprint arXiv:2009.03509*, 2020.
- [93] K. Kong, G. Li, M. Ding, Z. Wu, C. Zhu, B. Ghanem, G. Taylor, and T. Goldstein, "Flag: Adversarial data augmentation for graph neural networks," *arXiv preprint arXiv:2010.09891*, 2020.
- [94] W. Sun, W. Jiang, E. Trulls, A. Tagliasacchi, and K. M. Yi, "Acne: Attentive context normalization for robust permutation-equivariant learning," in *Proceedings of the IEEE/CVF Conference on Computer Vision and Pattern Recognition*, 2020, pp. 11 286–11 295.
- [95] Z. Yang, W. W. Cohen, and R. Salakhutdinov, "Revisiting semi-supervised learning with graph embeddings," *arXiv preprint arXiv:1603.08861*, 2016.
- [96] J. McAuley, C. Targett, Q. Shi, and A. Van Den Hengel, "Image-based recommendations on styles and substitutes," in *Proceedings of the 38th international ACM SIGIR conference on research and development in information retrieval*, 2015, pp. 43–52.
- [97] J. Tang, J. Sun, C. Wang, and Z. Yang, "Social influence analysis in large-scale networks," in *Proceedings of the 15th ACM SIGKDD international conference on Knowledge discovery and data mining*, 2009, pp. 807–816.



**Tianlong Chen** is a Ph.D. student in Electrical and Computer Engineering at University of Texas at Austin. He received his B.S. degree from University of Science and Technology of China in 2017. He has also interned at IBM Research, Facebook AI, Microsoft Research and Walmart Technology Lab. His research focuses sparse neural networks, AutoML, adversarial robustness, self-supervised learning and graph learning.



**Kaixiong Zhou** received the BS and MS degrees in electrical engineering and information science from Sun Yat-Sen University and University of Science and Technology of China, respectively. He is currently a Ph.D student in the Department of Computer Science at Rice University. His research interests include data mining, network analytics, and graph neural networks.



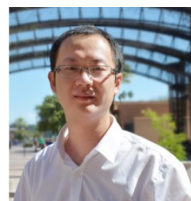
**Keyu Duan** is currently pursuing his Ph.D. degree in computer science with Rice University, supervised by Dr. Xia (Ben) Hu at DATA lab. Before that, he received the B.E. degree of Software Engineering from Beihang University, Beijing, China. His research interests include Network Analytics, Graph Neural Networks, Scalable Graph Representation Learning, Knowledge Graph Reasoning.



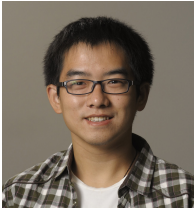
**Wenqing Zheng** received his B.Eng. degree in Communication Engineering from Beijing University of Posts and Telecommunications, China, in 2018, he received his M.S. in Eng. At the University of Texas at Austin in Dec. 2020. He is currently a Ph.D. student in the Department of Electrical and Computer Engineering at the University of Texas at Austin. His research interests include graph neural networks, transformers and and symbolic reasoning.



**Peihao Wang** is currently pursuing his Ph.D. degree in Electrical and Computer Engineering at the University of Texas at Austin. Prior to that, he received the B.E. degree of Computer Science from ShanghaiTech University, China, in 2020. His research interests focus on graph representation learning, 3D vision and graphics, and computational photography.



**Xia Hu** received the BS and MS degrees in computer science from Beihang University, China and the PhD degree in computer science and engineering from Arizona State University. He is currently an Associate Professor with the Department of Computer Science, Rice University. He has published nearly 100 papers in several major academic venues, including NeurIPS, ICLR, ICML, etc. His developed automated machine learning package, AutoKeras, has become the most rated open-source AutoML system.



**Zhangyang Wang** is currently an Assistant Professor of ECE at UT Austin. He received his Ph.D. in ECE from UIUC in 2016, and his B.E. in EEIS from USTC in 2012. Prof. Wang is broadly interested in the fields of machine learning, computer vision, optimization, and their interdisciplinary applications. His latest interests focus on automated machine learning (AutoML), learning-based optimization, machine learning robustness, and efficient deep learning.

## APPENDIX A MORE TECHNICAL DETAILS

**Diverse hyperparameter configurations of existing deep GNNs.** As shown in Table 12, 13, and 14, we can see that these highly inconsistent hyperparameter settings pose severely challenges to fairly compare the existing training tricks for deep GNNs.

TABLE 12  
Configurations adopted on Citeseer [44].

Methods	Total epoch	Learning rate & Decay	Weight decay	Dropout	Hidden dimension
Chen et al. (2020) [29]	100	0.01	5e-4	0.6	256
Xu et al. (2018) [12]	1000	0.005	5e-4	0.5	(16, 32)
Kilgus et al. (2018) [30]	10000	0.01	5e-3	0.5	64
Zhang et al. (2020) [31]	1500	(0.001, 0.005, 0.01)	-	{0.1, 0.2, 0.3, 0.4, 0.5}	64
Luan et al. (2019) [74]	3000	2.8218e-03	1.9812e-02	0.63277	5000
Liu et al. (2020) [33]	100	0.01	0.005	0.8	64
Zhao et al. (2019) [35]	100	0.005	5e-4	0.6	32
Min et al. (2020) [75]	200	0.005	0	0.9	-
Zhou et al. (2020) [12]	1000	0.005	5e-4	0.6	-
Zhou et al. (2020) [37]	50	0.005	1e-5	0	128
Rong et al. (2020) [34]	400	0.009	1e-3	0.8	128
Zou et al. (2020) [76]	100	0.001	-	-	256
Hasanzadeh et al. (2020) [77]	1700	0.005	5e-3	0	128

TABLE 13  
Configurations adopted on PubMed [44].

Methods	Total epoch	Learning rate & Decay	Weight decay	Dropout	Hidden dimension
Chen et al. (2020) [29]	100	0.01	5e-4	0.5	256
Kilgus et al. (2018) [30]	10000	0.01	5e-3	0.5	64
Zhang et al. (2020) [31]	1500	(0.001, 0.005, 0.01)	-	{0.1, 0.2, 0.3, 0.4, 0.5}	64
Luan et al. (2019) [74]	3000	0.001	0.02	0.63277	128
Liu et al. (2020) [33]	100	0.01	0.005	0.8	64
Zhao et al. (2019) [35]	1500	0.005	5e-4	0.6	(32, 64)
Zhou et al. (2020) [12]	1000	0.01	1e-3	0.6	-
Zhou et al. (2020) [37]	50	0.005	1e-5	0.5	128
Rong et al. (2020) [34]	400	0.009	1e-3	0.8	128
Zou et al. (2020) [76]	100	0.001	-	-	256
Hasanzadeh et al. (2020) [77]	2000	0.005	5e-3	0	128

TABLE 14  
Configurations adopted on Ogbn-ArXiv [23].

Methods	Total epoch	Learning rate & Decay	Weight decay	Dropout	Hidden dimension
Xu et al. (2018) [32]	500	0.01	-	0.5	128
Li et al. (2019, 2020) [19], [73]	500	0.01	-	0.5	128
Chen et al. (2020) [29]	1000	0.001	-	0.1	256
Zhang et al. (2020) [31]	1500	(0.001, 0.005, 0.01)	-	{0.1, 0.2, 0.3, 0.4, 0.5}	256
Liu et al. (2020) [33]	1000	0.005	-	0.2	256
Zhou et al. (2020) [37]	400	0.005	0.001	0.6	128
Zhou et al. (2020) [12]	2000	0.001	0.0005	0.3	128
Kong et al. (2020) [33]	500	0.01	-	0.5	256
Sun et al. (2020) [94]	2000	0.002	-	0.75	256

## APPENDIX B MORE IMPLEMENTATION DETAILS

**Datasets and computing facilities.** Table 15 provides the detailed properties and download links for all adopted datasets. We adopt the following benchmark datasets since i) they are widely applied to develop and evaluate GNN models, especially for deep GNNs studied in this paper; ii) they contains diverse graphs from small-scale to large scale or from homogeneous to heterogeneous; iii) they are collected from different applications including citation network, social network, etc. Specifically, the four datasets applied in benchmark studies are not the “small-world” graphs where any node can reach the other nodes in a few hops. The maximum diameters of strongly connected components in Cora, Citeseer, Pubmed, OGBN-arxiv are 19, 28, 18, and 23, respectively. The deep GNNs help encode the high-order neighborhood dependencies and the complex neighbor substructure for each node, which could boost the node classification tasks. All experiments on large graph datasets, e.g., OGBN-ArXiv, are conducted on single 48G Quadro RTX 8000 GPU. For other experiments on small graphs such as Cora, are ran at single 12G GTX 2080TI GPU. The detailed descriptions of these datasets are listed in the following.

- **Cora, Citeseer, Pubmed.** They are the scientific citation network datasets [44], [95], where nodes and edges represent the scientific publications and their citation relationships, respectively. Each node is described by bag-of-words representation, i.e., the 0/1-valued word vector indicating the absence/presence of the corresponding words in the scientific publication. Each node is associated with a one-hot label, where the node classification task is to predict what field the corresponding publication belongs to.

- **OGBN-Arxiv.** The OGBN-Arxiv dataset is a benchmark citation network collected in open graph benchmark (OGB) [23], which has been widely to evaluate GNN models recently. Each node represents an arXiv paper from computer science domain, and each directed edge indicates that one paper cites another one. The node is described by a 128-dimensional word embedding extracted from the title and abstract in the corresponding publication. Similar to Cora, Citeseer, and Pubmed, the node classification task is to predict the subject areas of the corresponding arXiv papers.
- **Coauthor CS, Coauthor Physics.** They are the co-authorship graph datasets [90] from the scientific fields of computer science and physics, respectively. The nodes represent the authors, and the links indicate whether the two corresponding nodes co-authored papers. Node features represent paper keywords for each author’s papers. The node classification task is to predict the most active fields of study for the corresponding author.
- **Amazon Computers, Amazon Photo.** These two datasets [90] are the segments of the Amazon co-purchase graph [96]. While nodes are the items, edges indicate whether the two items re frequently bought together or not. The node features are given by bag-of-words representations extracted from the product reviews, and the class labels denote the product categories.
- **Texas, Wisconsin, Cornell.** They are the three sub-datasets of WebKB (<http://www.cs.cmu.edu/afs/cs.cmu.edu/project/theo-11/www/wskb>) collected from computer science departments of various universities by Carnegie Mellon University [91]. While nodes represent webpages in the webpage datasets, edges are hyperlinks between them. The node feature vectors are given by bag-of-word representation of the corresponding webpages. Each node is associated with one-hot label to indicate one of the following five categories, i.e., student, project, course, staff, and faculty.
- **Actor.** This is an actor co-occurrence network, which is an actor-only induced subgraph of the film-director-actor-writer network [97]. In the actor co-occurrence network, nodes correspond to actors and edges denote the co-occurrence relationships on the same Wikipedia pages. Node feature vectors are described by bag-of-word representation of keywords in the actors’ Wikipedia pages. The node classification task is to predict the topic of the actor’s Wikipedia page.

**Backbone Details.** We implement backbones GCN (<https://github.com/tkipf/gcn>) and SGC (<https://github.com/Tiiiger/SGC>) to compare the different tricks as studied in Section 3. Specifically, we follow the official model implementations of GCN and SGC to evaluate tricks of graph normalization and random dropping. While the default dropout rate listed in Table 2 is applied for backbones (GCN/SGC+NoNorm) in benchmarking normalization techniques, the dropout rate is optimized from set {0.2, 0.5, 0.7} for backbones (GCN/SGC+Dropout) in benchmarking dropping methods. To evaluate the skip connections and identity mapping, we further include feature transformation layers to the initial and the end of backbones, which project initial

features into hidden embedding space and map hidden embeddings to node labels, respectively. The backbones are denoted by GCN/SGC+None and GCN+without in Tables 3 and 6, respectively. The slight adaptations over the backbones explain the different baseline performances for the benchmark studies of skip connections, graph normalization, random dropping, and others.

TABLE 15  
Graph datasets statistics and download links.

Dataset	Nodes	Edges	Avg. Degree	Features	Classes	Download Links
Corra	2,708	5,428	3.88	1,433	7	<a href="https://github.com/kimyoung/plantoid/raw/master/data">https://github.com/kimyoung/plantoid/raw/master/data</a>
Citeseer	3,327	4,732	2.84	3,703	6	<a href="https://github.com/kimyoung/plantoid/raw/master/data">https://github.com/kimyoung/plantoid/raw/master/data</a>
PubMed	19,717	44,338	4.50	500	3	<a href="https://github.com/kimyoung/plantoid/raw/master/data">https://github.com/kimyoung/plantoid/raw/master/data</a>
OCGIN-Arxiv	169,343	1,666,243	13.77	128	40	<a href="https://github.com/kimyoung/plantoid/raw/master/data">https://github.com/kimyoung/plantoid/raw/master/data</a>
Coauthor CS	18,533	81,894	8.93	6085	15	<a href="https://github.com/schuh/gnn-benchmark/raw/master/data/ocgin/">https://github.com/schuh/gnn-benchmark/raw/master/data/ocgin/</a>
Coauthor Physics	34,491	247,982	14.38	8,415	5	<a href="https://github.com/schuh/gnn-benchmark/raw/master/data/ocgin/">https://github.com/schuh/gnn-benchmark/raw/master/data/ocgin/</a>
Amazon Computers	13,383	245,278	36.74	767	5	<a href="https://github.com/schuh/gnn-benchmark/raw/master/data/ocgin/">https://github.com/schuh/gnn-benchmark/raw/master/data/ocgin/</a>
Amazon Photo	7,487	119,043	31.80	745	8	<a href="https://github.com/schuh/gnn-benchmark/raw/master/data/ocgin/">https://github.com/schuh/gnn-benchmark/raw/master/data/ocgin/</a>
Texas	183	309	3.38	1,703	5	<a href="https://github.com/ocgin/ocgin/blob/master/data/ocgin/">https://github.com/ocgin/ocgin/blob/master/data/ocgin/</a>
Wisconsin	183	499	5.45	1,703	5	<a href="https://github.com/ocgin/ocgin/blob/master/data/ocgin/">https://github.com/ocgin/ocgin/blob/master/data/ocgin/</a>
Cornell	183	295	3.22	1,703	5	<a href="https://github.com/ocgin/ocgin/blob/master/data/ocgin/">https://github.com/ocgin/ocgin/blob/master/data/ocgin/</a>
Actor	7,600	33,544	8.83	931	5	<a href="https://github.com/ocgin/ocgin/blob/master/data/ocgin/">https://github.com/ocgin/ocgin/blob/master/data/ocgin/</a>

APPENDIX C

MORE EXPERIMENTAL RESULTS

More results of skip connections. Table 16 collects the achieved test accuracy with different skip connection mechanisms, and the standard deviations of 100 independent runs are reported.

TABLE 16  
Test accuracy (%) with skip connection.

Backbone	Settings	Cora		Citeseer		PubMed		OCGIN-Arxiv	
		2	16	2	16	2	16	2	16
GCN	Baseline	74.73±1.41	78.41±0.46	19.97±4.94	64.81±1.17	20.71±1.27	58.64±1.30	58.74±1.17	60.16±0.50
	Initial	79.01±1.10	78.81±0.84	78.74±0.86	70.15±0.84	68.41±0.83	68.36±1.10	77.92±1.17	77.52±1.35
	Jumping	81.98±0.85	78.04±1.04	67.26±0.51	66.53±0.53	55.03±0.27	57.83±0.68	70.62±1.05	73.36±2.28
	Drop	79.86±1.17	69.49±1.43	67.26±0.51	68.18±1.93	48.35±7.79	41.48±5.27	72.53±2.64	69.91±0.49
	None	82.38±0.83	21.89±1.34	21.22±1.37	71.46±0.44	39.93±1.76	20.29±1.19	79.78±0.39	78.07±1.20
SGC	Baseline	81.77±0.28	83.85±0.41	80.14±0.40	71.68±0.33	71.31±0.37	71.03±0.49	78.97±0.28	69.96±0.23
	Initial	81.40±0.28	83.66±0.38	83.77±0.38	71.60±0.33	72.16±0.30	72.28±0.38	79.11±0.21	79.73±0.21
	Jumping	77.75±0.65	83.42±0.83	83.81±0.48	69.86±0.37	71.89±0.52	77.42±0.47	79.99±0.48	80.07±0.67
	Drop	77.11±0.39	81.24±1.12	77.66±1.74	79.94±0.58	75.15±1.85	63.51±5.12	74.84±1.18	78.18±0.28
	None	79.31±0.37	78.98±1.06	68.45±1.10	72.31±0.38	71.03±1.18	61.92±0.38	78.06±0.31	69.18±0.58

More results of graph normalizations. Table 17 reports the performance with different graph normalization techniques. The standard deviations are included.

TABLE 17  
Test accuracy (%) with graph normalization.

Backbone	Settings	Cora		Citeseer		PubMed		OCGIN-Arxiv	
		2	16	2	16	2	16	2	16
GCN	FullNorm	69.91±1.56	62.10±1.88	29.65±1.68	46.27±2.30	26.25±1.21	21.82±2.91	47.15±1.94	80.81±1.42
	PairNorm	74.41±1.36	82.79±1.19	17.67±0.21	63.26±1.12	27.48±2.37	20.67±0.51	75.87±0.86	71.30±1.50
	NodeNorm	79.87±0.50	78.02±0.51	21.40±0.91	48.90±1.02	18.11±1.12	19.03±1.33	73.14±0.79	40.10±0.29
	MeanNorm	82.05±0.35	13.57±1.14	13.01±0.15	70.96±0.36	16.79±0.30	78.60±0.41	18.92±0.20	18.01±0.03
	GroupNorm	62.41±0.53	41.76±1.07	27.20±1.13	71.30±1.46	26.75±0.74	28.82±0.78	78.98±0.48	68.84±0.28
SGC	FullNorm	80.00±0.86	51.64±1.23	21.44±2.57	68.99±1.03	18.50±1.27	18.51±1.68	78.11±0.28	40.10±0.28
	PairNorm	82.43±0.33	21.73±0.52	21.21±0.48	71.40±0.48	19.74±1.31	19.99±1.38	78.07±1.20	71.97±0.31
	NodeNorm	79.32±0.25	15.86±0.86	14.07±0.72	61.60±1.31	17.74±0.45	17.82±0.75	54.22±1.53	20.49±1.83
	MeanNorm	80.78±0.23	71.26±1.12	51.03±2.25	69.76±1.33	60.14±2.40	50.94±2.76	75.81±0.54	68.10±0.49
	GroupNorm	78.95±0.54	9.27±0.88	7.93±0.40	63.42±1.45	41.01±1.58	40.22±2.22	71.64±1.42	70.91±1.72

More results of random droppings. Table 18 shows the performance rates of random dropping tricks, where all dropout rates are reported for best test accuracies. Table 19 and 20 report the test accuracies with fixed dropout rates 0.2 and 0.5 respectively, for better comparison. For all experiments, the standard deviations of 100 independent repetitions are provided.

TABLE 18  
Test accuracy (%) with random dropping.

Dataset	Settings	Cora		Citeseer		PubMed		OCGIN-Arxiv	
		2	16	2	16	2	16	2	16
GCN	No Dropout	61.68±1.13	28.56±2.97	26.36±2.56	71.36±0.18	21.90±1.07	20.80±1.13	79.56±0.17	39.05±1.47
	Dropout	82.99±0.36	21.60±1.54	21.17±3.29	71.04±0.40	19.37±1.88	20.15±1.37	39.99±1.23	39.17±1.43
	DropRate	77.11±0.14	27.01±1.54	27.01±1.54	68.95±0.17	22.52±1.07	22.52±1.07	78.16±0.12	78.16±0.12
	DropEdge	79.16±0.73	28.03±1.36	27.97±3.04	70.20±0.70	23.92±1.12	23.92±1.12	76.58±0.58	40.11±1.20
	DropNode	77.02±0.18	28.03±1.36	27.97±3.04	70.20±0.70	23.92±1.12	23.92±1.12	76.58±0.58	40.11±1.20
SGC	No Dropout	81.20±0.75	22.34±0.30	18.13±0.40	70.90±0.00	24.09±0.60	18.23±0.55	78.85±0.04	44.41±1.23
	Dropout	77.11±0.14	27.01±1.54	27.01±1.54	68.95±0.17	22.52±1.07	22.52±1.07	78.16±0.12	78.16±0.12
	DropEdge	79.16±0.73	28.03±1.36	27.97±3.04	70.20±0.70	23.92±1.12	23.92±1.12	76.58±0.58	40.11±1.20
	DropNode	77.02±0.18	28.03±1.36	27.97±3.04	70.20±0.70	23.92±1.12	23.92±1.12	76.58±0.58	40.11±1.20
	DropRate	79.86±1.17	69.49±1.43	67.26±0.51	68.18±1.93	48.35±7.79	41.48±5.27	72.53±2.64	69.91±0.49

TABLE 19  
Test accuracy (%) with random dropping  $p = 0.2$ .

Dataset	Settings	Cora		Citeseer		PubMed		OCGIN-Arxiv	
		2	16	2	16	2	16	2	16
GCN	DropNode $p = 0.2$	77.10±1.04	27.01±1.54	27.01±1.54	68.95±0.17	22.52±1.07	22.52±1.07	78.16±0.12	78.16±0.12
	DropEdge $p = 0.2$	79.16±0.73	28.03±1.36	27.97±3.04	70.20±0.70	23.92±1.12	23.92±1.12	76.58±0.58	40.11±1.20
	DropRate $p = 0.2$	81.02±0.75	18.51±0.48	18.13±0.40	70.90±0.00	24.09±0.60	18.23±0.55	78.85±0.04	44.41±1.23
	DropEdge+Dropout $p = 0.2$	79.71±0.81	27.01±1.54	27.01±1.54	68.95±0.17	22.52±1.07	22.52±1.07	78.16±0.12	78.16±0.12
	LADRS+Dropout $p = 0.2$	78.88±0.76	19.49±1.31	18.62±0.60	69.02±0.68	27.17±0.74	18.54±2.38	78.53±0.77	41.43±2.28
SGC	DropNode $p = 0.2$	77.02±0.18	28.03±1.36	27.97±3.04	70.20±0.70	23.92±1.12	23.92±1.12	76.58±0.58	40.11±1.20
	DropEdge $p = 0.2$	79.16±0.73	28.03±1.36	27.97±3.04	70.20±0.70	23.92±1.12	23.92±1.12	76.58±0.58	40.11±1.20
	DropRate $p = 0.2$	79.86±1.17	69.49±1.43	67.26±0.51	68.18±1.93	48.35±7.79	41.48±5.27	72.53±2.64	69.91±0.49
	DropEdge+Dropout $p = 0.2$	79.86±1.17	69.49±1.43	67.26±0.51	68.18±1.93	48.35±7.79	41.48±5.27	72.53±2.64	69.91±0.49
	LADRS+Dropout $p = 0.2$	79.86±1.17	69.49±1.43	67.26±0.51	68.18±1.93	48.35±7.79	41.48±5.27	72.53±2.64	69.91±0.49

More results of comparison between previous state-of-the-art frameworks. We present a more complete comparison

TABLE 20  
Test accuracy (%) with random dropping  $p = 0.5$ .

Dataset	Settings	Cora		Citeseer		PubMed		OCGIN-Arxiv	
		2	16	2	16	2	16	2	16
GCN	DropNode $p = 0.5$	76.21±1.26	21.09±1.56	20.62±1.92	65.47±1.31	18.68±0.35	19.88±1.24	73.82±1.38	40.31±1.41
	DropEdge $p = 0.5$	76.91±1.15	21.07±1.24	20.57±2.43	65.39±1.30	20.48±1.28	20.87±1.07	73.21±1.39	40.11±1.28
	DropRate $p = 0.5$	79.86±1.17	69.49±1.43	67.26±0.51	68.18±1.93	48.35±7.79	41.48±5.27	72.53±2.64	69.91±0.49
	DropEdge+Dropout $p = 0.5$	76.91±1.15	21.07±1.24	20.57±2.43	65.39±1.30	20.48±1.28	20.87±1.07	73.21±1.39	40.11±1.28
	LADRS+Dropout $p = 0.5$	76.91±1.15	21.07±1.24	20.57±2.43	65.39±1.30	20.48±1.28	20.87±1.07	73.21±1.39	40.11±1.28
SGC	DropNode $p = 0.5$	76.08±0.24	63.92±1.19	29.10±1.46	71.83±0.26	27.21±1.41	19.97±0.18	77.65±0.31	48.97±1.24
	DropEdge $p = 0.5$	80.07±0.36	59.31±0.74	22.44±0.43	70.84±0.48	68.04±0.29	70.66±0.20	78.91±0.28	77.24±0.14
	DropRate $p = 0.5$	80.07±0.36	59.31±0.74	22.44±0.43	70.84±0.48	68.04±0.29	70.66±0.20	78.91±0.28	77.24±0.14
	DropEdge+Dropout $p = 0.5$	79.81±0.56	67.01±1.14	42.68±0.33	70.21±0.49	46.27±1.47	34.90±1.18	76.88±0.45	70.53±0.16
	LADRS+Dropout $p = 0.5$	79.81±0.56	67.01±1.14	42.68±0.33	70.21±0.49	46.27±1.47	34.90±1.18	76.88±0.45	70.53±0.16

TABLE 21  
Acc. (%) (100 runs) comparison with previous SOTAs.

Model	Cora (Ours: 85.48±0.39)		Citeseer (Ours: 73.35±0.79)		PubMed (Ours: 80.76±0.26)		OCGIN-Arxiv (Ours: 72.70±0.15)	
	2	16	2	16	2	16	2	16
SGC [31]	79.31±0.37	75.98±1.06	68.45±1.30	72.31±0.38	71.03±1.18	61.92±3.48	78.06±0.31	69.18±0.58
DAGNN [10]	80.31±0.78	84.14±0.39	83.39±0.59	18.22±3.48	73.05±0.62	72.99±0.54	77.44±0.57	80.58±0.51
GCN [14]	82.19±0.77	84.69±0.51	85.29±0.47	67.81±0.89	79.07±0.15	80.03±0.80	79.91±0.27	71.24±0.17
JKNet [10]	83.61±0.11	72.97±0.34	73.23±3.59	66.98±1.82	84.33±1.74	50.68±0.73	72.44±0.02	63.77±0.21
APPNP [10]	82.86±0.46	83.44±0.48	83.66±0.48	71.67±0.78	72.13±0.63	79.46±0.67	80.33±0.33	65.31±0.23
GPRGNN [10]	79.59±0.49	83.89±0.53	83.13±0.60	70.49±0.95	71.39±0.73	70.71±0.79	78.73±0.63	78.16±0.10
Ours	85.48±0.37	84.42±0.37	85.11±0.41	85.38±0.53	85.40±0.47	85.39±0.43	85.48±0.42	85.46±0.40

TABLE 22  
Cora with 2/4/8/16/32/64/128 GNNs from 100 runs.

Model	Cora (Ours: 85.48)						
	2	4	8	16	24	32	64
SGC	79.31±0.37	77.34±0.26	74.94±0.31	75.98±1.06	68		